

RAM: A Conserved Signaling Network That Regulates Ace2p Transcriptional Activity and Polarized Morphogenesis^D

Bryce Nelson,^{*†} Cornelia Kurischko,^{†‡} Joe Horecka,[§] Manali Mody,[‡]
Pradeep Nair,^{||} Lana Pratt,^{||} Alexandre Zougman,[¶] Linda D.B. McBroom,[¶]
Timothy R. Hughes,[#] Charlie Boone,^{*#@} and Francis C. Luca^{‡@}

^{*}Department of Biology Queen's University, Kingston, Ontario K7L 3N6, Canada; [†]Department of Animal Biology, University of Pennsylvania School of Veterinary Medicine, Philadelphia, Pennsylvania 19104; [§]DiscoveRx Corp., Fremont, CA 94538; ^{||}Institute of Molecular Biology and Biochemistry, Simon Fraser University, Burnaby, British Columbia V5A 1S6, Canada; [¶]MDS Proteomics Inc., Toronto, Ontario M9W 7H4, Canada; and [#]Banting and Best Department of Medical Research, University of Toronto, Toronto, Ontario M5S 1A8, Canada

Submitted January 17, 2003; Revised May 9, 2003; Accepted May 9, 2003
Monitoring Editor: Anthony Bretscher

In *Saccharomyces cerevisiae*, polarized morphogenesis is critical for bud site selection, bud development, and cell separation. The latter is mediated by Ace2p transcription factor, which controls the daughter cell-specific expression of cell separation genes. Recently, a set of proteins that include Cbk1p kinase, its binding partner Mob2p, Tao3p (Pag1p), and Hym1p were shown to regulate both Ace2p activity and cellular morphogenesis. These proteins seem to form a signaling network, which we designate RAM for regulation of Ace2p activity and cellular morphogenesis. To find additional RAM components, we conducted genetic screens for bilateral mating and cell separation mutants and identified alleles of the PAK-related kinase Kic1p in addition to Cbk1p, Mob2p, Tao3p, and Hym1p. Deletion of each RAM gene resulted in a loss of Ace2p function and caused cell polarity defects that were distinct from formin or polarisome mutants. Two-hybrid and coimmunoprecipitation experiments reveal a complex network of interactions among the RAM proteins, including Cbk1p–Cbk1p, Cbk1p–Kic1p, Kic1p–Tao3p, and Kic1p–Hym1p interactions, in addition to the previously documented Cbk1p–Mob2p and Cbk1p–Tao3p interactions. We also identified a novel leucine-rich repeat-containing protein Sog2p that interacts with Hym1p and Kic1p. Cells lacking Sog2p exhibited the characteristic cell separation and cell morphology defects associated with perturbation in RAM signaling. Each RAM protein localized to cortical sites of growth during both budding and mating pheromone response. Hym1p was Kic1p- and Sog2p-dependent and Sog2p and Kic1p were interdependent for localization, indicating a close functional relationship between these proteins. Only Mob2p and Cbk1p were detectable in the daughter cell nucleus at the end of mitosis. The nuclear localization and kinase activity of the Mob2p–Cbk1p complex were dependent on all other RAM proteins, suggesting that Mob2p–Cbk1p functions late in the RAM network. Our data suggest that the functional architecture of RAM signaling is similar to the *S. cerevisiae* mitotic exit network and *Schizosaccharomyces pombe* septation initiation network and is likely conserved among eukaryotes.

INTRODUCTION

The establishment and maintenance of cell polarity are critical for proper cellular function and development. Indeed, the importance of cell polarity is abundantly evident in a variety of cells, such as neurons and intestinal epithelial cells, for which polarized morphogenesis is es-

sential for their specialized functions (Andersen and Bi, 2000). The temporal and spatial regulation of cell polarity and morphogenesis seems to be highly complex, involving the integration of multiple signaling networks, includ-

Article published online ahead of print. Mol. Biol. Cell 10.1091/mbc.E03-01-0018. Article and publication date are available at www.molbiolcell.org/cgi/doi/10.1091/mbc.E03-01-0018.

^D Online version of this article contains supplementary data for

some figures. Online version is available at <http://www.molbiolcell.org>.

[†] These authors contributed equally to this work.

[@] Corresponding authors. E-mail addresses: fluca@vet.upenn.edu and charlie.boone@utoronto.ca.

ing those that regulate cell size and cell division (Knust, 2000; Rupes, 2002).

In the budding yeast *Saccharomyces cerevisiae*, multiple signaling networks coordinate bud emergence, polarized growth, and cell cycle progression (Pruyne and Bretscher, 2000a,b; Casamayor and Snyder, 2002). In response to favorable nutrient conditions, cell size, and initiation of cell cycle progression, a Ras-like GTPase signaling network becomes activated to specify the site of bud emergence. Coincident with initiation of DNA replication, the G1/S phase cyclin-dependent kinase (CDK) complex, Cln1/2p–Cdc28p, promotes bud emergence through activation of the Cdc42p GTPase cycle, which controls the assembly of macromolecular complexes containing multiple polarity determinant proteins (Lew and Reed, 1995; Pruyne and Bretscher, 2000a,b). In particular, the formin protein Bni1p controls the assembly of actin cables, which guide myosin-motor directed secretion (Evangelista *et al.*, 2002; Pruyne *et al.*, 2002; Sagot *et al.*, 2002). During the initial stages of bud development, secretion is polarized to the bud tip, such that growth is focused to the bud apex. Later in the cell cycle, a switch is made from apical to isotropic growth, such that secreted materials are directed uniformly over the entire surface of the developing bud. This switch correlates with the coupling of CDK to the mitotic cyclins, Clb1/2p, and subsequent activation of a network involving the Nim1-like kinase Gin4p and the PAK-like kinase Cla4p, which terminate Cdc42p signaling (Gulli *et al.*, 2000). At the end of mitosis, polarized cell growth is redirected from the bud cortex to the mother-daughter cell junction at the bud neck to facilitate septum formation and cell separation (Kilmartin and Adams, 1984).

The mechanisms involved in polarized growth in *S. cerevisiae* are also required for the formation of mating projections. Chemotropic growth of mating projections enables haploid cells of opposite mating types to make contact and subsequently form a diploid zygote through cell and nuclear fusion. Mating pheromone activates a cell surface G protein-coupled receptor, which stimulates a downstream mitogen-activated kinase pathway and Cdc42p-signaling to induce the expression of mating genes, G1 cell cycle arrest, and polarized secretion, leading to the formation of a mating projection or shmoo (Leberer *et al.*, 1997; Elion, 2000). Like polarized bud growth, formation of polarized mating projections requires Bni1p-mediated assembly of actin cables, which direct the secretion of plasma membrane and cell wall components to the growing tip of the cell (Evangelista *et al.*, 2002; Pruyne *et al.*, 2002; Sagot *et al.*, 2002).

The *S. cerevisiae* Mob2p–Cbk1p kinase complex has been implicated in the regulation of polarized growth during budding and mating (Colman-Lerner *et al.*, 2001; Weiss *et al.*, 2002). Cbk1p kinase belongs to a conserved family of serine-threonine protein kinases, whose members include Dbf2p, a component of the *S. cerevisiae* mitotic exit network (MEN), *S. pombe* Orb6 and Sid2, and mammalian Ndr and LATS kinases (Verde *et al.*, 1998; Racki *et al.*, 2000; Bardin and Amon, 2001; Bidlingmaier *et al.*, 2001). Cbk1p kinase activity peaks during periods of polarized bud growth and during late mitosis (Weiss *et al.*, 2002). Cbk1p activity is dependent on Mob2p, a member of the Mob family of proteins that includes Mob1p, a Dbf2p binding protein and component of the *S. cerevisiae* MEN (Luca and Winey, 1998; Weiss *et al.*,

2002). Cells deleted for either *CBK1* or *MOB2* are round, as are cells expressing a catalytically inactive form of Cbk1p (Racki *et al.*, 2000; Bidlingmaier *et al.*, 2001; Colman-Lerner *et al.*, 2001; Weiss *et al.*, 2002). Similarly, *S. pombe* mutant cells that lack *CBK1* and *MOB2* orthologs are round (Verde *et al.*, 1998; Hou *et al.*, 2003). The round cell morphology of *cbk1Δ* and *mob2Δ* mutants indicates a failure to establish or maintain apical bud growth. Consistent with a general role for the Mob2p–Cbk1p protein complex in polarized morphogenesis, *mob2Δ* and *cbk1Δ* mutants are defective in pheromone-induced projection formation (Bidlingmaier *et al.*, 2001; Weiss *et al.*, 2002). Moreover, the conditional inactivation of Cbk1p kinase results in the depolarization of the actin cytoskeleton at the growing tips of mating projections (Weiss *et al.*, 2002).

In addition to their role in polarized growth, Cbk1p and Mob2p are critical for regulating the localization and activity of Ace2p transcription factor, which mediates mother-daughter cell separation at the end of mitosis (Colman-Lerner *et al.*, 2001; Weiss *et al.*, 2002). In wild-type cells, Ace2p localizes to daughter cell nuclei during mitotic exit and activates a set of genes that are essential for mother-daughter cell separation, such as *CTS1* and *SCW11*, which encode proteins involved in septum degradation (Dohrmann *et al.*, 1992; Bidlingmaier *et al.*, 2001; Colman-Lerner *et al.*, 2001; Doolin *et al.*, 2001; Weiss *et al.*, 2002). Consistent with their dual roles in cell polarity and Ace2p regulation, Cbk1p and Mob2p localize to sites of cortical growth during G1 through mid-mitosis and to the bud neck region and the daughter cell nucleus at the end of mitosis (Colman-Lerner *et al.*, 2001; Weiss *et al.*, 2002). Cells deleted for *ACE2*, *CBK1*, or *MOB2* display similar cell separation defects; however, unlike *cbk1Δ* and *mob2Δ* mutant cells, *ace2Δ* cells are not defective in polarized morphogenesis (Racki *et al.*, 2000; Bidlingmaier *et al.*, 2001). Thus, the role of the Mob2p–Cbk1p protein complex in Ace2p regulation is distinct from its role in polarized morphogenesis.

The mechanism for Mob2p–Cbk1p kinase activation remains to be elucidated. However, given the sequence similarities between Mob1p and Mob2p and between their respective kinase partners, Dbf2p and Cbk1p, it is likely that the Mob2p–Cbk1p complex is activated within a signaling pathway whose circuitry resembles that of the *S. cerevisiae* MEN and *S. pombe* septation initiation network (SIN) (Bardin and Amon, 2001). So far, Hym1p, an ortholog of the *Aspergillus nidulans* hyphal growth protein hymA and the mouse MO25 protein (Miyamoto *et al.*, 1993; Karos and Fischer, 1999), and Tao3p (Pag1p), a 270 kDa protein conserved from yeast to humans of undefined molecular role, are the only known proteins that seem to function within the Mob2p–Cbk1p pathway (Dorland *et al.*, 2000; Bidlingmaier *et al.*, 2001; Du and Novick, 2002). However, Hym1p- and Tao3p-like proteins have not been implicated in MEN or SIN signaling.

Herein, we used a variety of approaches, including microarray analysis, protein–protein interaction methodologies, live cell microscopy, and in vitro kinase assays to investigate the functional relationships between Cbk1p, Mob2p, Tao3p, and Hym1p. We conducted genetic and two hybrid screens to identify additional genes involved in both polarized morphogenesis and cell separation. We present evidence that the serine-threonine kinase Kic1p (Sullivan *et*

al., 1998) and a novel leucine-rich repeat (LRR)-containing protein Sog2p collaborate with Cbk1, Mob2p, Tao3p, and Hym1p to regulate Ace2p transcriptional activity and polarized morphogenesis. Each of these proteins localizes similarly to sites of polarized growth and displays a complex array of physical interactions and interdependencies for subcellular localization, indicating an intimate functional relationship. Notably, we establish that Mob2p–Cbk1p activity is dependent on Kic1p, Tao3p, Hym1p, and Sog2p, and we provide evidence that Hym1p, Sog2p, and Kic1p interact to form a functional unit. Given the sequence similarity of Kic1p to the MEN kinase Cdc15p, which activates the Mob1p–Dbf2p kinase complex directly (Mah *et al.*, 2001), it is probable that Kic1p activates Mob2p–Cbk1p for regulating Ace2p and cellular morphogenesis.

MATERIALS AND METHODS

Yeast Strains and Culture Conditions

The yeast strains used in this study (Table 1) are derived from W303 (Evangelista *et al.*, 1997) or S288C (Roberts *et al.*, 2000; Weiss *et al.*, 2002) and were cultured as described previously. Strains deleted for *BNII* (Y3314), *CBK1* (Y1747), *MOB2* (Y3424), *TAO3* (Y3152), *HYM1* (Y1560), *KIC1* (Y3323), and *SOG2* (FLY1492), were created using a polymerase chain reaction (PCR)-based targeted gene replacement strategy, as described previously (Longtine *et al.*, 1998).

Cells expressing C-terminal-tagged proteins (3 × hemagglutinin [HA], 13 × Myc, or green fluorescent protein [GFP]) were constructed via PCR-based gene fusion, as described previously (Longtine *et al.*, 1998). These alleles did not cause any observable phenotypes, indicating that the tags did not interfere with protein function. Double mutant combinations were constructed through standard genetic crossing methods.

Identification of Bilateral Mating Mutants

Cells were engineered to select for mutants with reduced mating efficiency. Mutant *ade2Δ* cells grown in medium containing low levels of adenine are red, due to the accumulation of a red biosynthetic precursor of adenine (Ugolini and Bruschi, 1996). *ade2Δ ade8Δ* double mutants fail to accumulate the red pigment due to a blockage at an earlier step in biosynthesis and therefore grow as white colonies. In haploid cells, *a2* encodes a transcriptional repressor of *MATa*-specific genes. In diploid cells, *a1-α2* represses haploid-specific genes, such as *FUS1* and *HO*. *FUS1pr-ADE8* (*ADE8* behind the *FUS1* promoter) was used as a haploid-specific pheromone response reporter. When integrated into the genome of a haploid *ade2Δ ade8Δ* cells, the basal activation of *FUS1* expression is strong enough to produce adequate amounts of Ade8p, thus yielding red colonies. Colonies that successfully mate will produce diploid cells that will repress the production of *FUS1pr-ADE8* (due to *a1-α2* repression of haploid-specific genes) and therefore look white, due to a lack of production of Ade8p. Mutations in the pheromone response cascade repress the basal signaling of *FUS1* and thus yield white colonies. We selected for more subtle bilateral mating mutants that cannot mate efficiently and therefore continue to express *FUS1pr-ADE8*. Colonies of such mutants are red or contain red and white sectors when grown on adenine-deficient plates.

Strain Y282 (*MATa ade2Δ ade8Δ GAL1pr-MATα2, FUS1pr-ADE8*) was transformed with p1240, a YCp50 (CEN, *URA3*) plasmid containing *HO*, which encodes an endonuclease that catalyzes mating type conversion. Cells were grown in synthetic medium lacking uracil and containing 2% galactose and plated onto rich medium containing minimal amounts of adenine and 2% glucose. They were then immediately mutagenized with UV light to a 10% survival rate. Of the 20,000 colonies screened, 262 were chosen for further analysis based on a red sectoring quality. Colonies were streaked onto

5-fluoroorotic acid medium to counterselect for *HO* plasmid and assayed for mating type. *MATa* isolates were assayed for G1 arrest, by using a modified protocol from (Fink and Styles, 1972) and for pheromone production and response as described previously (Boone *et al.*, 1993). Of 262 colonies, 75 were found to be normal for these assays and subjected to further analysis. *FAR1* was transformed into these strains and found to complement 11, which were subsequently removed from further analysis. One of the mutants that showed a round cell morphology, and a cell separation defect (Y871) was transformed with a YCp50 (CEN, *URA3*)-based genomic library. Approximately 14,000 colonies were screened for restored mating ability. Plasmids were recovered and sequenced from cells exhibiting an increased mating efficiency. A single complementing plasmid clone was isolated (p1319) that contained the *HYM1* gene and flanking sequences. *HYM1* was subcloned and confirmed to complement the mutant phenotypes of Y871.

Isolation of Cell Separation Mutants

Y2862, which contains an integrated copy of *OCH1pr-HIS3* and *OCH1pr-lacZ*, was transformed with an mTn-3 × HA/GFP mutagenized library (Burns *et al.*, 1994) and plated onto synthetic medium lacking uracil and histidine and containing 15 mM 3-amino triazole. Colonies (340,000) were screened for growth on medium containing 15 mM 3-amino triazole, and 59 colonies were selected. Eight colonies of the 59 also exhibited a cell separation phenotype and round cell morphologies. These mutants were placed into four complementation groups and direct genomic sequencing was used to determine the identity and transposon insertion site of each of the mutants (Horecka and Jigami, 2000). Four alleles of *TAO3*, two alleles of *KIC1*, and single alleles of *MOB2* and *CBK1* were recovered. All mutations showed elevated *OCH1* expression (approximately twofold above wild type) by *lacZ* measurement (Horecka, unpublished data). Only *cbk1Δ* cells showed elevated levels of *OCH1* expression (twofold) by DNA microarray analysis, which illustrates the greater sensitivity of the *lacZ*-reporter for analysis of gene expression.

Suppression of Cell Separation Mutants

Y1614 (*hym1Δ::LEU2*), which is defective for cell separation, was transformed with the YEp24-based (*URA3*, 2 μ) genomic library. Approximately 18,000 colonies were pooled and placed vertically at room temperature for 40 min and allowed to sediment. A small volume (0.25 ml) of liquid was transferred from the culture and transferred to 50 ml of fresh SD-URA and grown at 30°C to saturation. This enrichment for nonsedimenting cells was repeated for two additional rounds. Liquid was taken from the surface of the culture and plated onto SD-URA at a density of ~200 colony-forming units/plate. Forty-nine round, smooth colonies were chosen for microscopic analysis to confirm cell separation. Plasmids were extracted and examined by restriction analysis, one was sequenced and found to contain a 10.8-kb insert containing *ACE2* (p3679).

DNA Microarrays

Yeast cultures were grown for three generations to mid-logarithmic phase in synthetic complete medium. Cells were pelleted and frozen in liquid nitrogen. RNA extractions and hybridizations were performed as described previously (Roberts *et al.*, 2000).

Assays for Development of Mating Projections

Logarithmically growing *MATa* cells were exposed to 50 nM synthetic α -factor for 2 h and stained with rhodamine-phalloidin to visualize filamentous actin. Cells were scored for ability to polarize filamentous actin patches to discrete sites at the tips of cells.

Table 1. Strain list

Name	Relevant Genotype	Source
SY2585	<i>MATa his3::FUS1-HIS3 mfa2Δ::FUS1-lacZ ura3-1 leu2-3,-112 trp 1-1 ade2-1 can 1-100</i>	Sprague lab
SY2625	<i>MATa bar 1Δhis3::FUS1-HIS3 mfa2Δ::FUS1-lacZ ura3-1 leu2-3,-112 trp1-1 ade2-1 can1-100</i>	Sprague lab
W303-1A	<i>MATa ura3-1 leu2-3,-112 his3-11,-15 trp1-1 ade2-1 can1-100</i>	
Y282	<i>MATa lys2Δ::FUS1-pADE8hoΔ::GAL1-α2 ade8Δ his3::FUS1-HIS3 mfa2Δ::FUS1-lacZ ura3-1 leu2-3,-112 trp1-1 ade2-1 can1-100</i>	This study
Y483	<i>MATa bni1Δ::URA3 his3::FUS1-HIS3 mfa2Δ::FUS1-lacZ ura3-1 leu2-3,-112 trp1-1 ade2-1 can1-100</i>	This study
Y580	<i>MATa spa2Δ::LEU2 trp1 his3::FUS1-HIS3 mfa2Δ::FUS1-lacZ ura3-1 leu2-3,-112 ade2-1 can1-100</i>	This study
Y581	<i>MATa bni1Δ::LEU2 trp1 his3::FUS1-HIS3 mfa2Δ::FUS1-lacZ ura3-1 leu2-3,-112 ade2-1 can1-100</i>	This study
Y587	<i>MATa bni1Δ::URA3 bar1::LEU2 trp1 his3::FUS1-HIS3 mfa2Δ::FUS1-lacZ ura3-1 leu2-3,-112 ade2-1 can1-100</i>	This study
Y773	<i>MATa bud6Δ::URA3 bar1 his3::FUS1-HIS3 mfa2Δ::FUS1-lacZ ura3-1 leu2-3,-112 trp1-1 ade2-1 can1-100</i>	This study
Y837	<i>MATa bud6Δ::LEU2 bar1 his3::FUS1-HIS3 mfa2Δ::FUS1-lacZ ura3-1 leu2-3,-112 trp1-1 ade2-1 can1-100</i>	This study
Y860	<i>MATα 8 LEXA operator-ADE2::URA3 ade2-1 his3-11,15 leu2-3,117 trp1-1</i>	Evangelista <i>et al.</i> (2000)
Y871	<i>MATa hym1 bar1Δ::LEU2 lys2Δ::FUS1-pADE8 hoΔ::GAL1-α2 ade8Δhis3::FUS1-HIS3 mfa2Δ::FUS1-lacZ ura3-1 leu2-3,-112 trp1-1 ade2-1 can1-100</i>	This study
Y1026	<i>MATa ura3::URA3-LexAop-LacZ ura3-1 leu2-3,-112 his3-11,-15 trp1-1 ade2-1 can1-100</i>	Evangelista <i>et al.</i> (2000)
Y1028	<i>MATa/α ura3-1 leu2-3,-112 his3-11,-15 trp1-1 ade2-1 can1-100</i>	This study
Y1560	<i>MATa hym1Δ::URA3 ura3-1 leu2-3,-112 his3-11,-15 trp1-1 ade2-1 can1-100</i>	This study
Y1603	<i>MATa hym1Δ::HIS3 ura3-1 leu2-3, 112 his3-11,-15 trp1-1 ade2-1 can1-100</i>	This study
Y1614	<i>MATa hym1Δ::LEU2 ura3-1 leu2-3, 112 his3-11,-15 trp1-1 ade2-1 can1-100</i>	This study
Y1622	<i>MATa/α hym1Δ::LEU2/hym1Δ::LEU2 ura3-1/ura3-1 leu2-3, 112/leu2-3, 112 his3-11,-15/his3-11,-15 trp1-1/trp1-1 ade2-1/ade2-1 can1-100/can1-100</i>	This study
Y1726	<i>MATa cbk1Δ::kanMX6 bar1Δ::LEU2 ura3-1 leu2-3,-112 trp1-1 can1-100</i>	R. Geyer
Y1744	<i>MATa hym1Δ::URA3 bar1Δ::LEU2 ura3-1 leu2-3,-112 can1-100 his3::FUS1-HIS3 mfa2Δ::FUS1-lacZ</i>	This study
Y1747	<i>MATa cbk1Δ::kanMX6 ura3-1 leu2-3,-112 can1-100 his3::FUS1-HIS3 ade2-1 mfa2Δ::FUS1 lacZ</i>	This study
Y1749	<i>MATa hym1::URA3 cbk1Δ::kanMX6 bar1Δ::LEU2 ura3-1 leu2-3,-112 trp1-1 ade2-1 can1-100</i>	This study
Y2619	<i>MATa/α bni1::kanMX6/bni1Δ::LEU2 trp1/trp1 his3::FUS1-HIS3 mfa2Δ::FUS1-lacZ ura3-1/ura3-1 leu2-3,-112/leu2-3,-112 ade2-1/ade2-1 can1-100/can1-100</i>	This study
Y2623	<i>MATa/α cbk1Δ::kanMX6/cbk1Δ::kanMX6 ura3-1/ura3-1 leu2-3,-112/leu2-3,-112 can1-100/can1-100 his3::FUS1-HIS3 mfa2Δ::FUS1-lacZ</i>	This study
Y2862	<i>MATa his3::OCH1-HIS3 mfa2-Δ1::OCH1-lacZ ura3-1 leu2-3,-112 his3-11,-15 trp1-1ΔFA ade2-1 can1-100</i>	This study
Y3152	<i>MATa tao3Δ::kanMX6 ura3-1 leu2-3,-112 his3-11,-15 trp1-1 ade2-1 can1-100</i>	This study
Y3280	<i>MATa CBK1-13myc::kanMX6 ura3-1 leu2-3,-112 his3-11,-15 trp1-1 ade2-1 can1-100</i>	This study
Y3320	<i>MATa ACE2-GFP::HIS3MX6 ura3-1 leu2-3,-112 his3-11,-15 trp1-1 ade2-1 can1-100</i>	This study
Y3323	<i>MATa kio3Δ::kanMX6 ura3-1 leu2-3,-112 his3-11,-15 trp1-1 ade2-1 can1-100</i>	This study
Y3382	<i>MATa KIC1-GFP::HIS3MX6 ura3-1 leu2-3,-112 his3-11,-15 trp1-1 ade2-1 can1-100</i>	This study
Y3424	<i>MATa mob2Δ::kanMX6 ura3-1 leu2-3,-112 his3-11,-15 trp1-1 ade2-1 can1-100</i>	This study
Y3481	<i>MATa tao3Δ::kanMX6 bar1Δ::LEU2 ura3-1 leu2-3,-112 his3-11,-15 ade2-1 can1-100</i>	This study
Y3482	<i>MATa mob2Δ::kanMX6 bar1Δ::LEU2 ura3-1 leu2-3,-112 his3-11,-15 ade2-1 can1-100 lys2</i>	This study
Y3487	<i>MATa kic1Δ::kanMX6 bar1Δ::LEU2 ura3-1 leu2-3,-112 his3-11,-15 trp1-1 ade2-1 can1-100 lys2</i>	This study
Y3527	<i>MATa/α mob2Δ::kanMX6/mob2Δ::kanMX6 bar1Δ::LEU2/BAR1 ura3-1/ura3-1 leu2-3,-112/leu2-3,-112 his3-11,-15/his3-11,-15 trp1-1/trp1-1 ade2-1/ade2-1 can1-100/can1-100</i>	This study
Y3529	<i>MATa/α kic1Δ::kanMX6/kic1Δ::kanMX6 bar1Δ::LEU2/BAR1 ura3-1/ura3-1 leu2-3,-112/leu2-3,-112 his3-11,-15/his3-11,-15 trp1-1/trp1-1 ade2-1/ade2-1 can1-100/can1-100 lys2/LYS2</i>	This study
Y3565	<i>MATa/α tao3Δ::kanMX6/tao3Δ::kanMX6 bar1Δ::LEU2/BAR1 ura3-1/ura3-1 leu2-3,-112/leu2-3,-112 his3-11,-15/his3-11,-15 trp1-1/trp1-1 ade2-1/ade2-1 can1-100/can1-100 lys2/LYS2</i>	This study
Y3606	<i>MATa kic1Δ::kanMX6 cbk1Δ::kanMX6 bar 1Δ::LEU2 ura3-1 leu2-3,-112 trp1-1 ade2-1 can1-100 lys2</i>	This study
Y3608	<i>MATa hym1Δ::URA3 mob2Δ::kanMX6 bar1Δ::LEU2 ura3-1 leu2-3,-112 trp1-1 ade2-1 can1-100</i>	This study
Y3609	<i>MATa hym1Δ::URA3 tao3Δ::kanMX6 bar1Δ::LEU2 ura3-1 leu2-3,-112 trp1-1 ade2-1 can1-100</i>	This study
Y3615	<i>MATa KIC1 - HAx3::kanMX6 ura3-1 leu2-3,-112 his3-11,-15 trp1-1 ade2-1 can1-10</i>	This study
Y3625	<i>MATa kic1Δ::kanMX6 mob2Δ::kanMX6 bar1Δ::LEU2 ura3-1 leu2-3,-112 trp1-1 ade2-1 can1-100 lys2</i>	This study
Y3626	<i>MATa mob2Δ::kanMX6 cbk1Δ::kanMX6 bar1Δ::LEU2 ura3-1 leu2-3,-112 trp1-1 ade2-1 can1-100 lys2</i>	This study
Y3627	<i>MATa tao3Δ::kanMX6 cbk1Δ::kanMX6 bar1Δ::LEU2 ura3-1 leu2-3,-112 trp1-1 ade2-1 can1-100 lys2</i>	This study
Y3628	<i>MATa hym1Δ::URA3 kic1Δ::kanMX6 bar1Δ::LEU2 ura3-1 leu2-3,-112 trp1-1 ade2-1 can1-100</i>	This study
Y3644	<i>MATa tao3Δ::kanMX6 kic1Δ::kanMX6 bar1Δ::LEU2 ura3-1 leu2-3,-112 trp1-1 ade2-1 can1-100</i>	This study
Y3645	<i>MATa tao3Δ::kanMX6 mob2Δ::kanMX6 bar1Δ::LEU2 ura3-1 leu2-3,-112 trp1-1 ade2-1 can1-100 lys2</i>	This study
Y4032	<i>MATa CBK1-13myc::HIS3MX6 hym1Δ::URA3 ura3-1 leu2-3,-112 his3-11,-15 ade2-1 can1-100 trp1-1</i>	This study
Y4033	<i>MATa CBK1-13myc::HIS3MX6 tao3Δ::kanMX6 ura3-1 leu2-3,-112 his3-11,-15 ade2-1 can1-100 trp1-1</i>	This study
Y4034	<i>MATa CBK1-13myc::HIS3MX6 kic1Δ::kanMX6 ura3-1 leu2-3,-112 his3-11,-15 ade2-1 can1-100 trp1-1</i>	This study
Y4035	<i>MATa CBK1-13myc::HIS3MX6 mob2Δ::kanMX6 ura3-1 leu2-3,-112 his3-11,-15 ade2-1 can1-100 trp1-1</i>	This study

(continued)

Table 1. (Continued)

Name	Relevant Genotype	Source
Y4089	<i>MATa HYM1-13myc::kanMX6 KIC1 - HAx3::kanMX6 ura3-52 leu2-3, 112 trp1Δ1 his3Δ200</i>	This study
Y4122	<i>MATa ACE2 - GFP::HIS3MX6 cbk1Δ::kanMX6 ura3-1 leu2-3,-112 his3-11,-15 ade2-1 can1-100 lys2</i>	This study
FLY811	<i>MATa ACE2-GFP::kanMX6 ura3-52 leu2-3,-112 trp1Δ1 his3Δ200</i>	Weiss et al. (2002) S
FLY849	<i>MATa ACE2-GFP::kanMX6 mob2Δ::HIS3 ura3-52 leu2-3,112 trp1Δ1 his3Δ200</i>	Weiss et al. (2002) S
FLY853	<i>MATa ACE2-GFP::kanMX6 cbk1Δ::HIS3MX6 ura3-52 leu2-3,112 trp1Δ1 his3Δ200</i>	Weiss et al. (2002) S
FLY891	<i>MATa HYM1-GFP::kanMX6 ura3-52 leu2-3,112 trp1Δ1 his3Δ200</i>	Weiss et al. (2002) S
FLY893	<i>MATa/α MOB2-GFP::kanMX6/MOB2-GFP::HIS3MX6 ura3-52/ura3-52 leu2-3,112/leu2-3,112 trp1Δ1/trp1Δ1 his3Δ200/his3Δ200/</i>	Weiss et al. (2002) S
FLY895	<i>MATa/α CBK1-GFP::KANMX/CBK1-GFP::kanMX6 ura3-52/ura3-52 leu2-3, 112/leu2-3, 112 trp1Δ1/trp1Δ1 his3Δ200/his3Δ200</i>	Weiss et al. (2002) S
FLY947	<i>MATa KIC1-GFP::kanMX6 ura3 leu2-3,112 trp1 his3</i>	This study
FLY1081	<i>MATa ACE2-GFP::kanMX6 hym1Δ::URA3 ura3 leu2-3,112 trp1 his3</i>	This study
FLY1124	<i>MATa ACE2-GFP::kanMX6 tao3Δ::kanMX6 ura3-52 leu2-3,112 trp1Δ1 his3Δ200</i>	This study
FLY1134	<i>MATa ACE2-GFP::kanMX6 kic1Δ::kanMX6 ura3-52 leu2-3,112 trp1Δ1 his3Δ200</i>	This study
FLY1244	<i>MATa/α HYM1-GFP::kanMX6/HYM1-GFP::kanMX6 ura3-52/ura3-52 leu2-3,112/leu2-3,112 trp1Δ1/trp1Δ1 his3Δ200</i>	This study
FLY1245	<i>MATa/αHYM1-GFP::kanMX6/HYM1-GFP::kanMX6 mob2Δ::HIS3/mob2Δ::HIS3 ura3-52/ura3-52 leu2-3,112/leu2-3,112 trp1Δ1/trp1Δ1 his3Δ200/his3Δ200</i>	This study
FLY1246	<i>MATa/α HYM1-GFP::kanMX6/HYM1-GFP::kanMX6 cbk1Δ::HIS3MX6/cbk1Δ::HIS3MX6 ura3-52/ura3-52 leu2-3,112/leu2-3,112 trp1Δ1/trp1Δ1 his3Δ200/his3Δ200</i>	This study
FLY1247	<i>MATa/α KIC1-GFP::kanMX6 mob2Δ::HIS3 ura3-52/ura3-52 leu2-3,112/leu2-3,112 trp1Δ1/trp1Δ1 his3Δ200/his3Δ200</i>	This study
FLY1248	<i>MATa/αKIC1-GFP::kanMX6/KIC1-GFP::kanMX6 cbk1Δ::HIS3MX6/cbk1Δ::HIS3MX6 ura3-52/ura3-52 leu2-3,112/leu2-3,112 trp1Δ1/trp1Δ1 his3Δ200/his3Δ200</i>	This study
FLY1249	<i>MATa/α KIC1-GFP::kanMX6/KIC1-GFP::kanMX6 tao3Δ::kanMX6/tao3Δ::kanMX6 ura3/ura3 leu2-3,-112/leu2-3,112 trp1/trp1 his3/his3</i>	This study
FLY1258	<i>MATa/α KIC1-GFP::kanMX6/KIC1-GFP::kanMX6 ura3-52/ura3-52 leu2-3,112/leu2-3,112 trp1Δ1/trp1Δ1 his3Δ200/his3Δ200</i>	This study
FLY1259	<i>MATa/α CBK1-GFP::kanMX6/CBK1-GFP::kanMX6 tao3Δ::kanMX6/tao3Δ::kanMX6 ura3/ura3 leu2-3,-112/leu2-3,112 trp1/trp1 his3/his3</i>	This study
FLY1260	<i>MATa/α MOB2-GFP::HIS3MX6/MOB2-GFP::HIS3MX6 tao3Δ::kanMX6/tao3Δ::kanMX6 ura3/ura3 leu2-3,-112/leu2-3,112 trp1/trp1 his3/his3</i>	This study
FLY1261	<i>MATa/α HYM1-GFP::kanMX6/HYM1-GFP::kanMX6 kic1Δ::kanMX6/kic1Δ::kanMX6 ura3/ura3 leu2-3,-112/leu2-3,112 trp1/trp1 his3/his3</i>	This study
FLY1262	<i>MATa/α HYM1-GFP::kanMX6/HYM1-GFP::kanMX6 tao3Δ::kanMX6/tao3Δ::kanMX6 ura3/ura3 leu2-3,-112/leu2-3,112 trp1/trp1 his3/his3</i>	This study
FLY1263	<i>MATa TAO3-GFP::kanMX6 ura3-52 leu2-3, 112 trp1Δ1 his3Δ200</i>	This study
FLY1267	<i>MATa/α TAO3-GFP::HIS3MX6/TAO3-GFP::HIS3MX6 ura3-52/ura3-52 leu2-3,112/leu2-3,112 trp1Δ1/trp1Δ1 his3Δ200/his3Δ200</i>	This study
FLY1268	<i>MATa CBK1-13myc::HIS3MX6 ace2Δ::kanMX6 ura3-1 leu2-3,-112 his3-11,-15 trp1-1 ade2-1 can1-100</i>	This study
FLY1278	<i>MATa/α KIC1-GFP::kanMX6/KIC1-GFP::kanMX6 hym1Δ::URA3/hym1Δ::URA3 ura3/ura3 leu2-3,-112/leu2-3,112 trp1/trp1 his3/his3</i>	This study
FLY1324	<i>MATa/α TAO3-GFP::HIS3MX6/TAO3-GFP::HIS3MX6 cbk1Δ::kanMX6/cbk1Δ::kanMX6 ura3-52/ura3-52 leu2-3,112/leu2-3,112 trp1Δ1/trp1Δ1 his3Δ200/his3Δ200</i>	This study
FLY1325	<i>MATa/α TAO3-GFP::HIS3MX6/TAO3-GFP::HIS3MX6 kic1Δ::kanMX6/kic1Δ::kanMX6 ura3/ura3 leu2-3,-112/leu2-3,112 trp1/trp1 his3/his3</i>	This study
FLY1326	<i>MATa/α TAO3-GFP::HIS3MX6/TAO3-GFP::HIS3MX6 hym1Δ::URA3/hym1Δ::URA3 ura3/ura3 leu2-3,-112/leu2-3,112 trp1/trp1 his3/his3</i>	This study
FLY1342	<i>MATa/α MOB2-GFP::HIS3MX6/MOB2-GFP::HIS3MX6 hym1Δ::URA3/hym1Δ::URA3 ura3/ura3 leu2-3,-112/leu2-3,112 trp1/trp1 his3/his3</i>	This study
FLY1343	<i>MATa/α MOB2-GFP::HIS3MX6/MOB2-GFP::HIS3MX6 kic1Δ::kanMX6/kic1Δ::kanMX6 ura3/ura3 leu2-3,-112/leu2-3,112 trp1/trp1 his3/his3</i>	This study
FLY1344	<i>MATa/α CBK1-GFP::kanMX6 kic1Δ::kanMX6 ura3/ura3 leu2-3,-112/leu2-3,112 trp1/trp1 his3/his3</i>	This study
FLY1347	<i>MATa SOG2-GFP::kanMX6 ura3-52 leu2-3,112 trp1Δ1 his3Δ200</i>	This study
FLY1382	<i>MATa/α SOG2-GFP::kanMX6/SOG2-GFP::kanMX6 ura3-52/ura3-52 leu2-3,112/leu2-3,112 trp1Δ1/trp1Δ1 his3Δ200/his3Δ200</i>	This study
FLY1383	<i>MATa/α CBK1-GFP::kanMX6/CBK1-GFP::kanMX6 hym1Δ::URA3/hym1Δ::URA3 ura3/ura3 leu2-3,-112/leu2-3,112 trp1/trp1 his3/his3</i>	This study
FLY1386	<i>MATa/α TAO3-GFP::HIS3MX6/TAO3-GFP::HIS3MX6 mob2Δ::HIS3/mob2Δ::HIS3 ura3-52/ura3-52 leu2-3,112/leu2-3,112 trp1Δ1/trp1Δ1 his3Δ200/his3Δ200</i>	This study
FLY1465	<i>MATa/α KIC1-GFP::kanMX6/KIC1-GFP::kanMX6 sog2Δ::kanMX6/sog2Δ::kanMX6 ura3-52/ura3-52 leu2-3,112/leu2-3,112 trp1Δ1/trp1Δ1 his3Δ200/his3Δ200</i>	This study

(continued)

Table 1. (Continued)

Name	Relevant Genotype	Source
FLY1470	<i>MATα Ace2-GFP::kanMX6 sog2Δ::kanMX6 ura3-52 leu2-3,112 trp1Δ1 his3Δ200</i>	This study
FLY1471	<i>MATα/α SOG2-GFP::kanMX6/SOG2-GFP::kanMX6 kic1Δ::kanMX6/kic1Δ::kanMX6 ura3-52/ura3-52 leu2-3,112/leu2-3,112 trp1Δ1/trp1Δ1 his3Δ200/his3Δ200</i>	This study
FLY1472	<i>MATα/α SOG2-GFP::kanMX6/SOG2-GFP::kanMX6 hym1Δ::URA3/hym1Δ::URA3 ura3-52/ura3-52 leu2-3,112/leu2-3,112 trp1Δ1/trp1Δ1 his3Δ200/his3Δ200</i>	This study
FLY1473	<i>MATα/α SOG2-GFP::kanMX6/SOG2-GFP::kanMX6 tao3Δ::kanMX6/tao3Δ::kanMX6 ura3-52/ura3-52 leu2-3,112/leu2-3,112 trp1Δ1/trp1Δ1 his3Δ200/his3Δ200</i>	This study
FLY1474	<i>MATα/α SOG2-GFP::kanMX6/SOG2-GFP::kanMX6 mob2Δ::HIS3/mob2Δ::HIS3 ura3-52/ura3-52 leu2-3,112/leu2-3,112 trp1Δ1/trp1Δ1 his3Δ200/his3Δ200</i>	This study
FLY1475	<i>MATα/α SOG2-GFP::kanMX6/SOG2-GFP::kanMX6 cbk1Δ::HIS3 ura3-52/ura3-52 leu2-3,112/leu2-3,112 trp1Δ1/trp1Δ1 his3Δ200/his3Δ200</i>	This study
FLY1492	<i>MATα CBK1 CBK1-13myc::HIS3MX6 sog2Δ::kanMX6 ura3-1 leu2-3,-112 his3-11,-15 ade2-1 can1-100 trp1-1</i>	This study
FLY1499	<i>MATα/α MOB2-GFP::HIS3MX6/MOB2-GFP::HIS3MX6 sog2Δ::kanMX6/sog2Δ::kanMX6 ura3/ura3 leu2-3,-112/leu2-3,112 trp1/trp1 his3/his3</i>	This study
FLY1500	<i>MATα/α TAO3-GFP::HIS3MX6/TAO3-GFP::HIS3MX6 sog2Δ::kanMX6/sog2Δ::kanMX6 ura3/ura3 leu2-3,-112/leu2-3,112 trp1/trp1 his3/his3</i>	This study
FLY1514	<i>MATα/α HYM1-GFP::kanMX6/HYM1-GFP::kanMX6 sog2Δ::kanMX6/sog2Δ::kanMX6 ura3-52/ura3-52 leu2-3,112/leu2-3,112 trp1Δ1/trp1Δ1 his3Δ200/his3Δ200</i>	This study
FLY1515	<i>MATα/α CBK1-GFP::kanMX6/CBK1-GFP::kanMX6 sog2Δ::kanMX6/sog2Δ::kanMX6 ura3-52/ura3-52 leu2-3,112/leu2-3,112 trp1Δ1/trp1Δ1 his3Δ200/his3Δ200</i>	This study

Analysis of Budding Patterns

Strains expressing a *BUD4*-containing plasmid (p2698; a gift from Silvia Sanders, Massachusetts Institute of Technology, Cambridge, MA) or the vector pRS316 were grown in medium lacking uracil to mid-logarithmic phase. Cells were sonicated for cell separation and Calcofluor White was added to 2 μg/ml concentration. Bud scars were visualized by fluorescence microscopy and bud patterns were defined as described previously (Chant and Pringle, 1995). Only cells containing three or more bud scars were counted. Bud scars residing on opposite thirds of the cells were considered to be bipolar. Bud patterns were considered axial only if scars resided immediately adjacent to one another.

Cells were considered to have random patterns if bud scars resided in the middle third of the cell.

Two-Hybrid Screens and Assays

Two-hybrid bait and prey plasmids are listed in Table 2 and were based on pEG202, which encodes the LexA-DNA binding domain, and pJG4-5, which encodes the B42 transcriptional activation domain (Gyuris *et al.*, 1993). DNA fragments of various genes were amplified by the PCR with primers that incorporated 5'-*Bam*HI and 3'-*Not*I restriction sites (unless otherwise noted in Table 2) for insertion into the two-hybrid vectors.

Two-hybrid assays were performed as described previously (Phizicky and Fields, 1995) by mating Y1026, which contains a LexA DNA-binding domain plasmid, and Y860, which contains a prey plasmid. Diploids were grown on selective media and subjected to β-galactosidase expression analysis (Sheu *et al.*, 2000). Strains qualitatively more reactive than the vector control were classified as positive. p2139 was used as bait to identify genes encoding Hym1p-binding proteins from a yeast cDNA library derived from pACT (Durfee *et al.*, 1993). Plasmids encoding positive interactors were recovered and sequenced. One plasmid, designated p3153, contained a fragment of YOR353c (*SOG2*).

Plasmid Construction

To construct yeast strain Y282, several integrating plasmids (p40, p65 and p89) were created. The plasmid p40 introduces a frame-shift mutation at codon 45 of *ADE8* and was created in a three-step process. First, a 2-kb *Eco*RI-*Hind*III *ADE8* fragment was cloned into Ylplac211 (*URA3*; Gietz and Sugino, 1988) to create p23. p23 was cut with *Eco*RI and *Sna*BI, treated with Klenow and dNTPs, and religated to remove an *Msc*I site. The resultant plasmid, designated p38, was cut with *Eco*47III-*Hpa*I and ligated to a *Bam*HI linker (5'-CGG-GATCCCG-3') to create an *ADE8* frame-shift mutation. This plasmid (p40) was cut with *Msc*I to target integration to the *ADE8* locus.

p65 was used to integrate *GAL1-α2* at the *HO* locus, thereby disrupting *HO* after codon 83. It was constructed by cutting Ylplac211 with *Pvu*II to remove the multicloning site. A *Hind*III linker (5'-CCCAAGCTTGGG-3') was then ligated to create p41, which

Table 2. Two-hybrid plasmids

Plasmid name	Insert	Vector
p2139	Hym1p (1–300) XhoI	pEG202 XhoI
p3411	Cbk1p (1–347) XhoI	pEG202 XhoI
p3412,	Cbk1p (1–112) XhoI	pEG202 XhoI
p4424	Kic1p (1–282) BglIII	pEG202 BamHI
p4429	Tao3p (1–510) XhoI	pEG202 XhoI
p4434	Tao3p (1141–1775) XhoI	pEG202 XhoI
p4437	Tao3p (1776–2377) XhoI	pEG202 XhoI
p4445	Tao3p (1776–2377) XhoI	pEG202 XhoI
p2872	Cbk1p (1–756)	pJG4-5
p3413	Cbk1p (346–756)	pJG4-5
p3415	Cbk1p (1–347)	pJG4-5
p3416	Cbk1p (1–117)	pJG4-5
p4422	Mob2p (1–326)	pJG4-5
p4423	Kic1p (1–282) BglIII	pJG4-5 BamHI
p4426	Kic1p (283–1081) BglIII	pJG4-5 BamHI
p4428	Tao3p (1–510)	pJG4-5
p4431	Tao3p (511–1140)	pJG4-5
p4433	Tao3p (1141–1775)	pJG4-5
p4436	Tao3p (1776–2377)	pJG4-5

was subsequently cut with *HindIII* and ligated to a *HindIII* fragment carrying *HO* and its promoter, creating p53. p53 was cut with *PstI-BamHI* and ligated with an oligonucleotide linker containing *EcoRI-SstI* sites; the resultant plasmid was cut with *EcoRI* and *SstI* and ligated to a *EcoRI-SstI* fragment containing the *GAL1* promoter (p113, Boone laboratory collection) and a *BamHI-SstI* fragment containing a *MAT α 2* PCR product. The *MAT α 2* fragment was PCR amplified from genomic DNA by using primers AAAGGATCCA AAATGAGAAC GGCCGTA and AAAGAGCTCT TGGAAAAATC CATTAAC, which incorporate *BamHI* and *SstI* sites at the 5' and 3' ends, respectively.

p89 was used to introduce the *FUS1pr-ADE8* reporter was constructed as follows. A YIp plasmid containing a 4.8 Kb *LYS2* genomic fragment (pCP6; provided by Eric Foss, Fred Hutchinson Cancer Research Center, Seattle, WA), was digested with *HpaI* and ligated to linkers to introduce *HindIII-SrfI-XbaI* sites within the *LYS2* gene. The resultant plasmid (p72) was cut with *HindIII* and *XbaI* and ligated to the *HindIII-NheI* fragment of *FUS1pr-ADE8* from a pUC13-based plasmid (p51), to create p89.

The human MST3 gene was cloned from a pool of infant brain, placenta, spinal chord, and colon total RNAs (BD Biosciences Clontech, Palo Alto, CA) by reverse transcription-PCR by using the primers CGCGGATATC ACCATGGCTC ACTCCCCGGT GCA and CGCGGTCGAC GTGGGATGAA GTTCTCCAC CACT. The PCR fragment was ligated into *EcoRV* and *SaII*-digested pCMV-TAG 4A (Stratagene, La Jolla, CA), which resulted in a C-terminal FLAG-tagged MST3 cDNA under the control of the cytomegalovirus promoter, creating pMST3-FLAG.

Yeast Immunoprecipitation and Protein Kinase Assays

For coprecipitation experiments, 1-liter culture of yeast cells was grown to early log phase in rich media, and extracts were prepared by grinding frozen cell pellets in lysis buffer (0.1% Triton X-100, 50 mM Tris-HCl, 100 mM NaCl, 10 mM EDTA) containing a protease inhibitor cocktail (Roche Diagnostics, Indianapolis, IN). Immunoprecipitations were carried out with 1.5-ml extracts, containing 20–25 mg/ml total protein, monoclonal antibody HA.11 (Babco, Richmond, CA), or monoclonal antibody c-Myc (Babco) and G-Sepharose beads (Pharmacia, Peapack, NJ). Total yeast extract (25 μ g) was analyzed on immunoblots, and 10 and 90% of the immunoprecipitated material was analyzed for detection of the immunoprecipitated and coprecipitating proteins, respectively. Immunoblot analysis was performed as described previously (Peter *et al.*, 1993) and probed using rabbit polyclonal HA antibody (Babco) and rabbit polyclonal c-Myc antibody (Santa Cruz Biotechnology, Santa Cruz, CA).

For Cbk1p protein kinase assays, cells were grown to mid-log phase and synchronized in G1 phase with mating pheromone. Cell extracts were prepared by glass bead lysis as described previously (Weiss *et al.*, 2002). Cell extracts were normalized to 5 mg/ml and immunoprecipitated by incubating in 4 μ g of anti-Myc antibody (9E10) for 45 min at 4°C followed by 25 μ l of Gamma-bind G-Sepharose (Pharmacia) for 45 min at 4°C. Immunoprecipitated material was washed four times in lysis buffer and three times in kinase buffer (50 mM HEPES pH 7.4, 60 mM sodium acetate, 10 mM MgCl₂, 1 mM dithiothreitol). Half the immunoprecipitated protein was processed for SDS-PAGE and immunoblotted. The other half was incubated in kinase buffer containing 5 μ g of histone H1, 10 μ M ATP, and 10 μ Ci of ³²P-ATP for 30 min at 30°C. Kinase reactions were terminated by addition of protein sample buffer and were processed for PAGE and autoradiography. Relative kinase activity was determined using a GS-525 PhosphorImager (Bio-Rad, Hercules, CA) and Multianalyst software.

Fluorescence Microscopy

Live cell microscopy was performed as described previously (Luca *et al.*, 2001; Weiss *et al.*, 2002).

RESULTS

CBK1, MOB2, TAO3, HYM1, and KIC1 Function in the Same Signaling Network

To identify *S. cerevisiae* genes that are required for polarized morphogenesis during both budding and mating, we performed two different genetic screens. First, we used a screen designed to uncover mutations that caused decreased efficiency in bilateral mating and defects in the formation of mating projections (see MATERIALS AND METHODS). From this screen, we identified an allele of *HYM1* that exhibited cell separation and round cell morphology defects, similar to that reported for *hym1 Δ* cells (Dorland *et al.*, 2000; Bidlingmaier *et al.*, 2001). Second, we screened for other mutations that cause cell separation and morphogenesis defects and identified alleles of *CBK1*, *MOB2*, *TAO3*, and *KIC1*. *KIC1* encodes a protein kinase that interacts with centrin-related Cdc31p and controls polarized growth and cell wall integrity (Sullivan *et al.*, 1998; Vink *et al.*, 2002). *HYM1*, *CBK1*, *MOB2*, *TAO3*, and *KIC1* are all essential for viability in the S288C-derived strain that was used by the yeast deletion consortium (Winzeler *et al.*, 1999). However, in our laboratory isolates of S288C (Luca laboratory) and W303 yeast strains (Luca and Boone laboratories), none of the genes is essential, which is likely due to a mutation in the *SSD1* gene (Du and Novick, 2002; Jorgensen *et al.*, 2002). We found that viable *hym1 Δ* , *cbk1 Δ* , *mob2 Δ* , *tao3 Δ* , and *kic1 Δ* deletion cells exhibit indistinguishable round cell morphology and cell separation defects (Figure 1) and fail to mate efficiently (our unpublished data).

Yeast cell separation requires the activation of Ace2p transcription factor, which controls the daughter cell-specific expression of genes required for septum degradation, such as *CTS1* and *SCW11* (Dohrmann *et al.*, 1992; Racki *et al.*, 2000; Colman-Lerner *et al.*, 2001; Doolin *et al.*, 2001). Ace2p localizes to the daughter cell nucleus at the end of mitosis (Colman-Lerner *et al.*, 2001; Weiss *et al.*, 2002), and its activation and daughter-specific localization are dependent on Mob2p and Cbk1p (Colman-Lerner *et al.*, 2001; Weiss *et al.*, 2002). In *tao3 Δ* , *hym1 Δ* and *kic1 Δ* cells, we found that Ace2p-GFP was not restricted to the daughter cell nucleus at the end of mitosis, but localized weakly to both mother and daughter cell nuclei (Figure 1), as observed in *mob2 Δ* and *cbk1 Δ* cells (Weiss *et al.*, 2002; Figure 1). These findings suggest that Mob2p, Cbk1p, Tao3p, Hym1p, and Kic1p function within the same signaling network, which we have designated the RAM network for regulation of Ace2p activity and cellular morphogenesis.

CBK1, MOB2, TAO3, HYM1, and KIC1 Are Essential for Ace2p-dependent Transcription

Ace2p is required for the daughter cell-specific transcription of a specific subset of genes (Colman-Lerner *et al.*, 2001). The gene expression profiles of *cbk1 Δ* cells were shown to be similar to *ace2 Δ* cells (Bidlingmaier *et al.*, 2001). To determine whether Mob2p, Tao3p, Hym1p, and Kic1p control the expression of a similar set of genes, we monitored global changes in gene expression for *cbk1 Δ* , *mob2 Δ* , *tao3 Δ* , *hym1 Δ* , and *kic1 Δ* cells

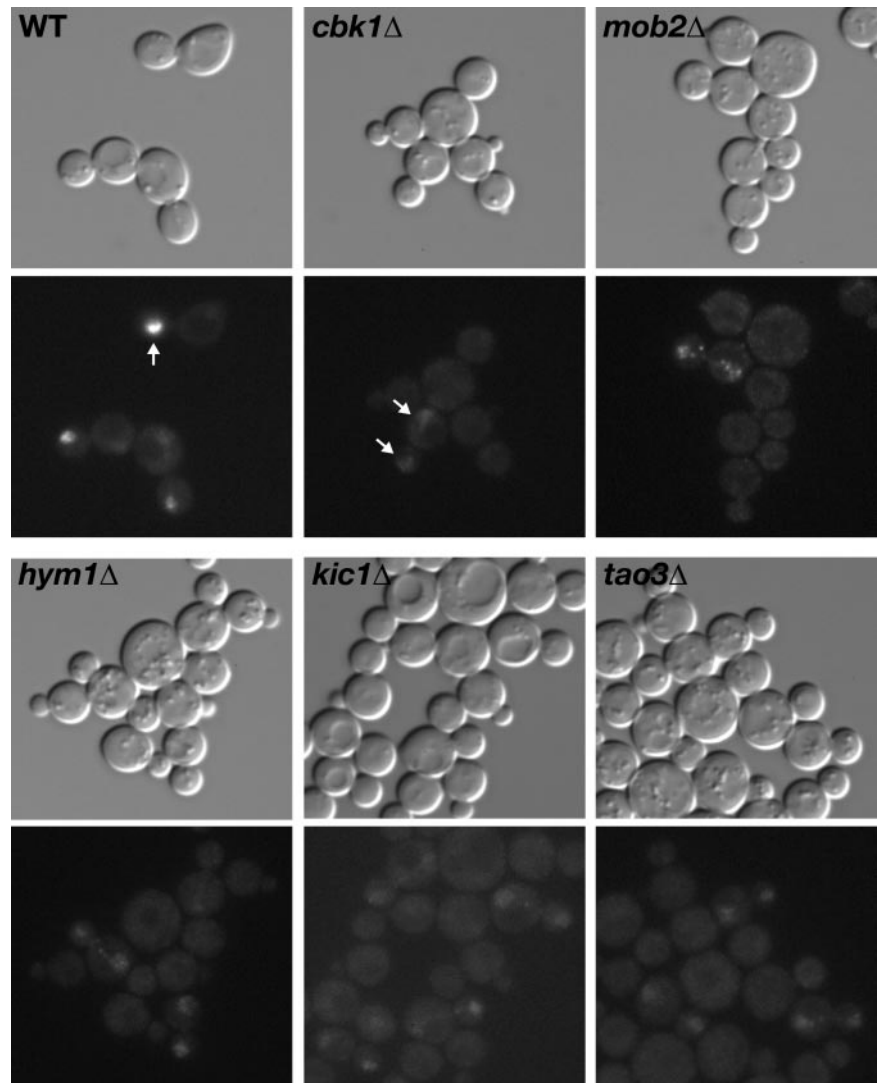


Figure 1. RAM deletion mutants are round in morphology and are defective for cell separation and Ace2p localization. Logarithmically growing wild-type (FLY811), *hym1Δ* (FLY1081), *cbk1Δ* (FLY853), *tao3Δ* (FLY1124), *kic1Δ* (FLY1134), and *mob2Δ* (FLY849) cells expressing *Ace2*-GFP were visualized by differential interference contrast microscopy (top) and fluorescence microscopy (bottom). Arrows point to *Ace2*-GFP in the nuclei of representative cells. Note that the relative fluorescence of *Ace2*-GFP in the nuclei of RAM mutants is weaker than in the daughter cell nuclei of wild-type cells. Morphological and cell separation phenotypes were not affected by *Ace2*-GFP expression (our unpublished data). All images were captured and processed identically.

during vegetative growth by microarray analysis (DeRisi *et al.*, 1997; Roberts *et al.*, 2000). We compared the gene expression profiles of the RAM network deletion mutants to a compendium of >300 reference gene expression profiles (Hughes *et al.*, 2000). We found that the expression profiles associated with *cbk1Δ*, *mob2Δ*, *tao3Δ*, *hym1Δ*, and *kic1Δ* were highly similar and formed a unique cluster (Figure 2). In particular, several *Ace2p*-regulated genes, such as *CTS1*, *SCW11*, and *DSE1*, *DSE2*, *DSE3*, and *DSE4* (Colman-Lerner *et al.*, 2001; Doolin *et al.*, 2001) were coregulated across numerous experiments and were dependent on Cbk1p, Mob2p, Tao3p, Hym1p, and Kic1p for normal expression (Figure 2). Thus, all of these proteins function in a common signaling pathway that controls *Ace2p* function.

***CBK1*, *MOB2*, *TAO3*, *HYM1*, and *KIC1* Are Required for Polarized Growth**

The round cell morphologies of *cbk1Δ*, *mob2Δ*, *tao3Δ*, *hym1Δ*, and *kic1Δ* cells suggest that, in addition to *Ace2p* regulation,

Cbk1p, Mob2p, Tao3p, Hym1p, and Kic1p have roles in polarized morphogenesis. To examine the roles of these proteins in pheromone-induced morphogenesis, we exposed *cbk1Δ*, *mob2Δ*, *tao3Δ*, *hym1Δ*, and *kic1Δ* cells to saturating levels of pheromone for 2 h and stained with rhodamine-phalloidin to visualize the filamentous actin cytoskeleton. Each of the five mutants formed broader and less pronounced mating projections than wild-type cells (Figure 3A), as observed for *cbk1Δ* and *mob2Δ* cells (Bidlemaier *et al.*, 2001; Weiss *et al.*, 2002). Only ~70% of the mutant cells, in contrast to ~98% of the wild-type cells, displayed a polarized distribution of cortical actin patches (Figure 3, A and B). Double mutant cells carrying different combinations of *cbk1Δ*, *mob2Δ*, *tao3Δ*, *hym1Δ*, and *kic1Δ* displayed defects in mating projection formation that were comparable to single mutants (Figure 3C). In contrast, similarly treated cells lacking the formin gene *BNI1* exhibited more severe defects in mating projection formation than *cbk1Δ*, *mob2Δ*, *tao3Δ*, *hym1Δ*, and *kic1Δ* single mutants or double mutants

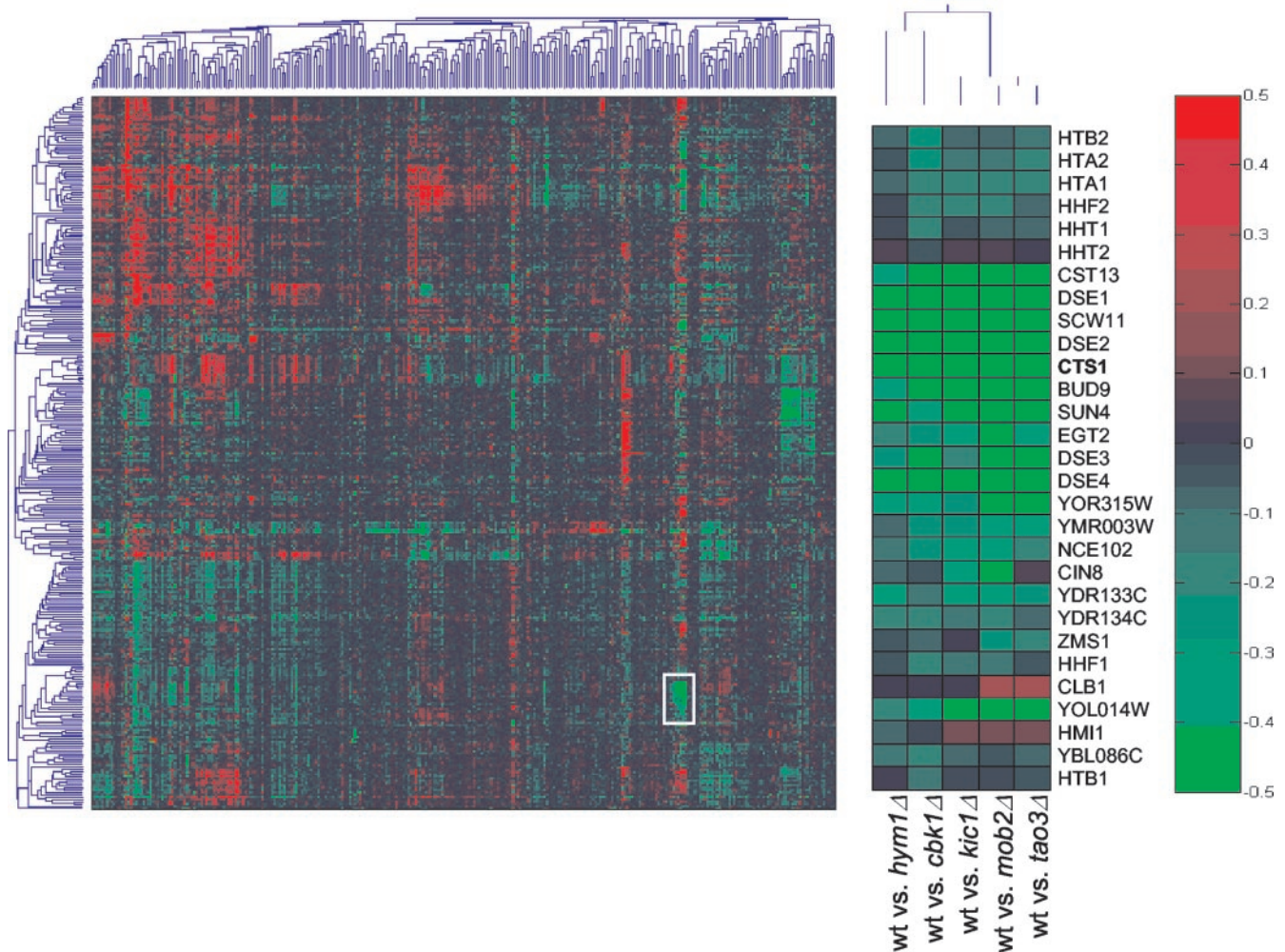


Figure 2. DNA microarray analysis of RAM deletion mutants. DNA microarray analysis of *hym1Δ* (Y1614), *cbk1Δ* (Y1726), *tao3Δ* (Y3152), *kic1Δ* (Y3323), and *mob2Δ* (Y3424) cells show overlapping expression profiles. Logarithmically growing cells were harvested or treated with 50 nM α -factor for 2 h before harvesting. Cells growing for vegetative profiling were grown in synthetic media containing all amino acids, cells treated with α -factor were grown in rich media. Two-dimensional clustering of DNA microarray profiles is presented. Gene expression is measured on a color scale (\log_{10}) with increased gene induction (red) or repression (green) corresponding to increased intensity. A gene cluster corresponding to Ace2p regulated genes is enlarged from the two-dimensional clustering for detailed examination (middle).

(Figure 3B). Significantly, cells lacking one of the RAM genes in combination with *bni1Δ* exhibited more severe defects in mating projection formation than single mutants (Figure 3D). Thus, Cbk1p, Mob2p, Tao3p, Hym1p, and Kic1p seem to collaborate to control cell polarity and likely function independently from Bni1p, which is required for actin cable assembly during polarized morphogenesis.

During budding, the cyclin-dependent kinase Cdc28p promotes polarized apical growth when coupled to the G1 cyclins and isotropic growth when coupled to mitotic cyclins (Lew and Reed, 1995). The apical growth phase can be prolonged by G1 cyclin overexpression, resulting in hyperelongated buds. Cells deleted for genes encoding cell polarity proteins, such as Bni1p, Bud6p and Spa2p (Chenevert *et al.*, 1994; Amberg *et al.*, 1997; Evangelista *et al.*, 1997; Sheu *et al.*, 1998), do not form hyperelongated

buds in response to overexpression of the G1 cyclin *CLN1*, presumably due to a defect in actin-dependent polarized secretion to the bud tip (Sheu *et al.*, 2000). To test Cbk1p, Mob2p, Tao3p, Hym1p, and Kic1p for a role in apical growth during budding, we overexpressed *CLN1* in deletion strains and scored for the presence of hyperelongated buds. With prolonged *CLN1* expression, wild-type cells showed a steady increase in the percentage of hyperelongated buds, reaching 55% of the total population after 4 h (Figure 4). In contrast, large budded *cbk1Δ*, *mob2Δ*, *tao3Δ*, *hym1Δ*, and *kic1Δ* cells resembled *bni1Δ*, *bud6Δ*, or *spa2Δ* cells, showing no apparent hyperelongation of buds and displayed a random distribution of actin patches. Immunoblot analysis revealed that the mutants and wild-type cells expressed comparable levels of galactose-induced Cln1p (our unpublished data). Thus, Cbk1p, Mob2p,

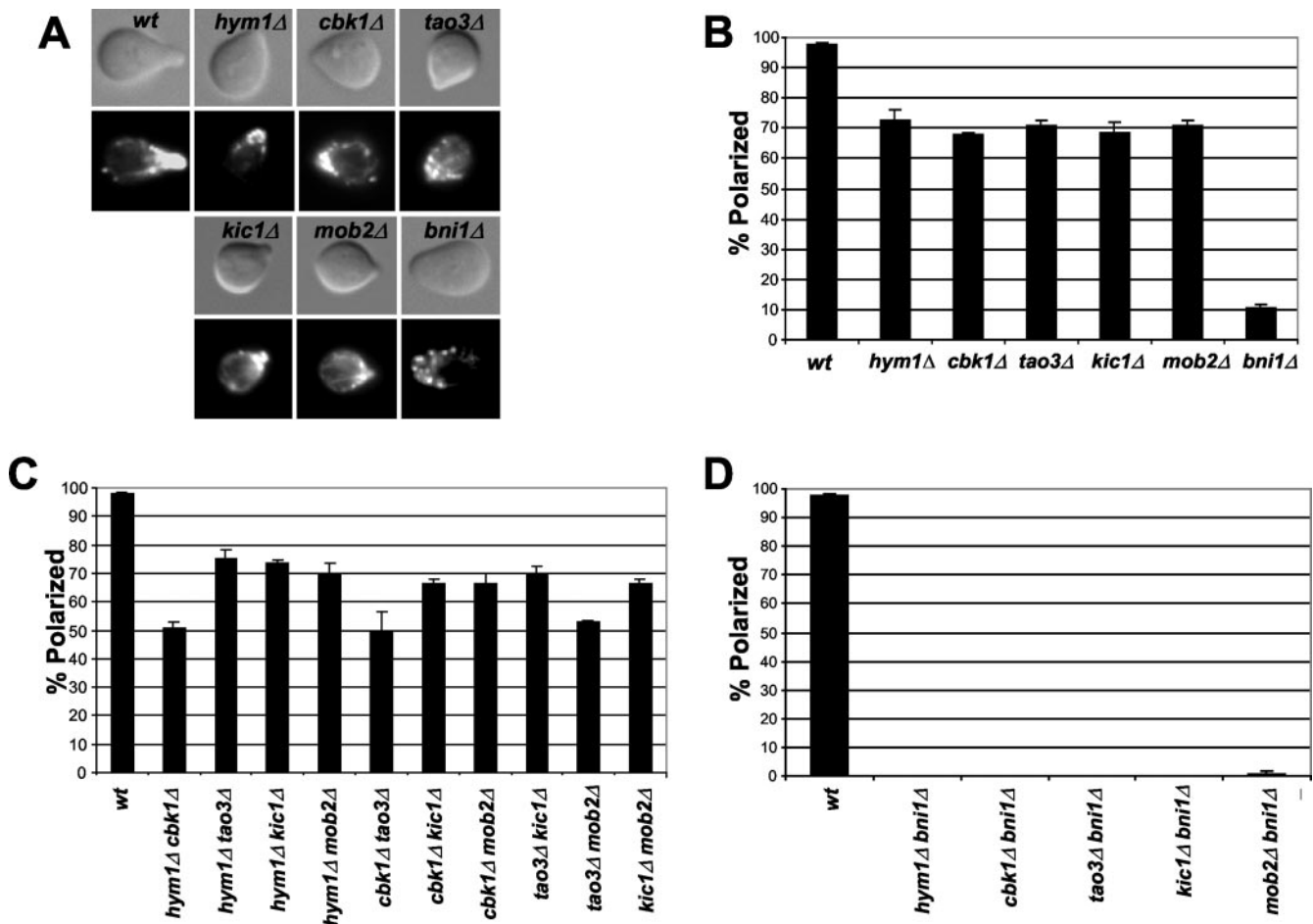


Figure 3. *HYM1*, *CBK1*, *TAO3*, *KIC1*, and *MOB2* are necessary for formation of mating projections. Logarithmically growing cells were treated with 50 nM α -factor for 2 h and stained with rhodamine-phalloidin to visualize filamentous actin. (A) Representative micrographs are shown of cells that successfully formed mating projections. Cells were treated with rhodamine-phalloidin for detecting F-actin. Top, differential interference contrast microscopy; bottom, fluorescence microscopy. (B) Wild-type, *hym1Δ*, *cbk1Δ*, *tao3Δ*, *kic1Δ*, and *mob2Δ* and *bni1Δ* cells were scored for their ability to form mating projections. (C) RAM double mutants in combination with *bni1Δ* were scored for their ability to form mating projections. (D) Cells harboring RAM gene deletions in combination with *bni1Δ* were scored for their ability to form mating projections. More than 100 cells were scored in three separate counts. Strains used were wild type (SY2625), *hym1Δ* (Y1744), *cbk1Δ* (1726), *tao3Δ* (3481), *kic1Δ* (3487), *mob2Δ* (3482), *bni1Δ* (Y587), *hym1Δcbk1Δ* (Y1749), *hym1Δtao3Δ* (Y3609), *hym1Δkic1Δ* (Y3628), *hym1Δmob2Δ* (Y3608), *cbk1Δtao3Δ* (Y3627), *cbk1Δkic1Δ* (Y3606), *cbk1Δmob2Δ* (Y3626), *tao3Δkic1Δ* (Y3644), *tao3Δmob2Δ* (Y3645), and *kic1Δmob2Δ* (Y3625).

Tao3p, Hym1p, and Kic1p are all required for the establishment or maintenance of apical bud growth.

HYM1, *CBK1*, *TAO3*, *KIC1*, and *MOB2* Affect Budding Patterns

Cells that are defective in actin-based polarized morphogenesis often display errors in bipolar bud site selection (Casamayor and Snyder, 2002). We examined the budding patterns of diploid *cbk1Δ*, *mob2Δ*, *tao3Δ*, *hym1Δ*, or *kic1Δ* cells that contained three or more calcofluor-stained bud scars. For wild-type diploids, 76% of the cells displayed bipolar budding patterns, whereas only 5–9% of diploid *cbk1Δ*, *mob2Δ*, *tao3Δ*, *hym1Δ*, and *kic1Δ* cells showed a bipolar pattern (Table 3). We also examined the budding patterns of haploid cells. The yeast strain W303 exhibits an axial bud-

ding defect, which can be rescued by introducing a plasmid carrying *BUD4* (our unpublished data). Approximately 83% of haploid W303 cells that were transformed with *pBUD4* showed an axial pattern (Table 3). In contrast, all five RAM deletion mutants exhibited reduced axial budding (Table 3). Only 55, 44, 56, 64, and 40% of *cbk1Δ*, *mob2Δ*, *tao3Δ*, *hym1Δ*, and *kic1Δ* cells, respectively, displayed axial budding patterns. Thus, Cbk1p, Mob2p, Tao3p, Hym1p, and Kic1p are not essential for axial budding but seem to participate in this process.

Cbk1p Kinase Activity Is Dependent on *Mob2p*, *Tao3p*, *Hym1p*, and *Kic1p*

Cbk1p kinase activity is critical for cell separation and maintenance of polarized growth (Racki *et al.*, 2000; Colman-

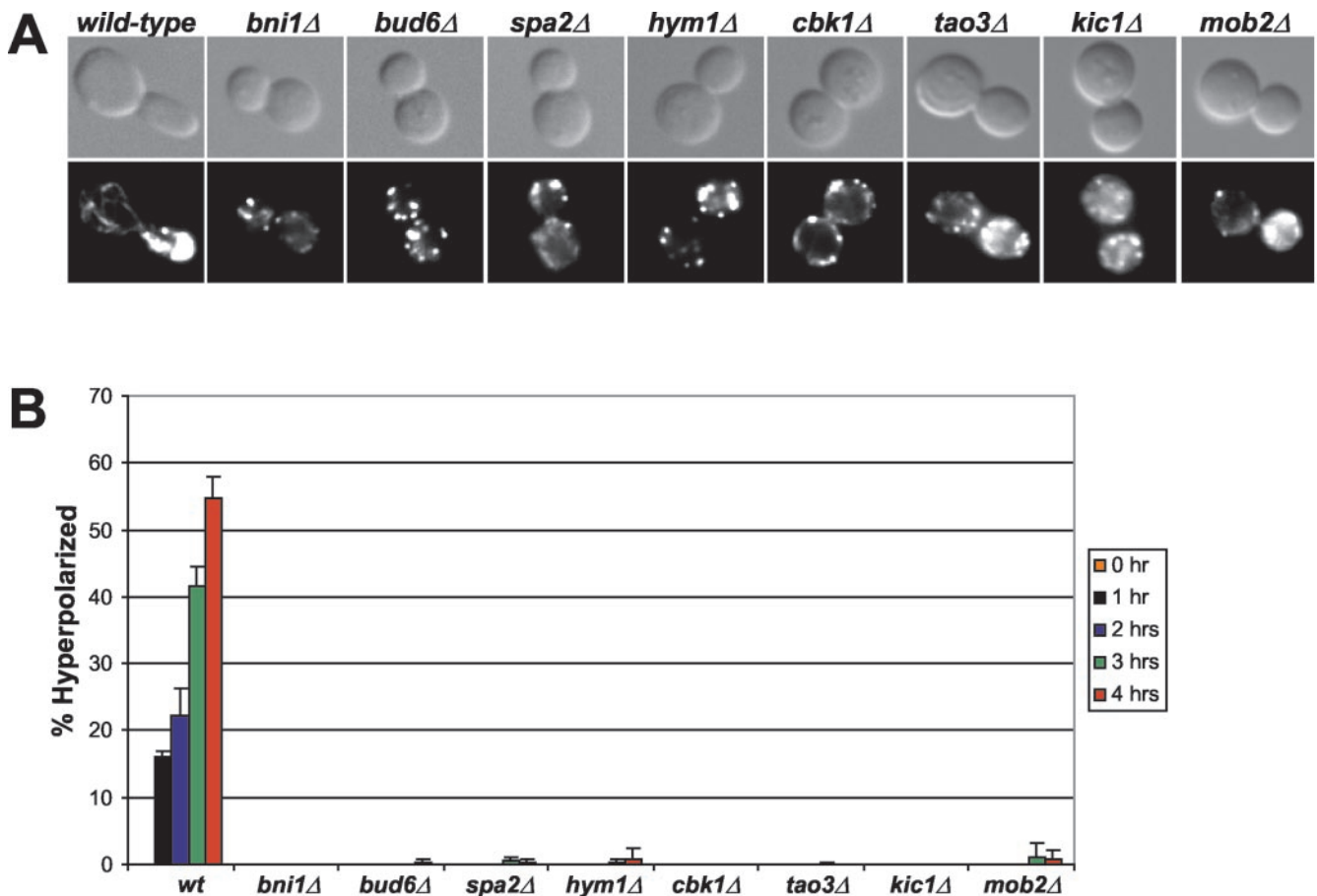


Figure 4. *HYM1*, *CBK1*, *TAO3*, *KIC1*, and *MOB2* are important for apical growth. (A) Cells overexpressing *GAL1pr-CLN1* are shown. Top, differential interference contrast microscopy; bottom, fluorescence microscopy. Strains containing *GAL1-CLN1* were induced by addition of galactose and stained with rhodamine-phalloidin to visualize filamentous actin. (B) Cells were scored for bud hyperelongation over time. Scoring consisted of counting >100 cells three independent times. The strains used were wild type (W3031A), *bni1Δ* (Y581), *bud6Δ* (Y837), *spa2Δ* (Y580), *hym1Δ* (Y1603), *cbk1Δ* (Y1747), *tao3Δ* (Y3152), *kic1Δ* (Y3323), and *mob2Δ* (Y3424). pMT485, containing *GAL1pr-CLN1* with the epitope tag HAx3 was provided by Mike Tyers (Samuel Lunenfeld Research Institute, Toronto, Ontario, Canada).

Lerner *et al.*, 2001; Weiss *et al.*, 2002) and thus may be a marker for RAM network activation. In agreement, Cbk1p kinase activity is stimulated during periods of polarized growth and peaks during late mitosis (Weiss *et al.*, 2002). Moreover, Cbk1p activation requires Mob2p (Weiss *et al.*, 2002). To test whether other RAM proteins are important for Cbk1p kinase activation, we immunoprecipitated Cbk1-Myc from pheromone-treated *ace2Δ*, *mob2Δ*, *tao3Δ*, *hym1Δ*, *kic1Δ*, and wild-type cells and performed *in vitro* kinase reactions by using histone H1 as substrate. Immunoblots revealed that similar amounts of Cbk1-Myc immunoprecipitated from *ace2Δ*, *tao3Δ*, *hym1Δ*, *kic1Δ*, and wild-type cells, whereas the amount of Cbk1-Myc immunoprecipitated from *mob2Δ* cells was more variable, ranging from equivalent to twofold less than that from wild-type cells (Figure 5). *In vitro* kinase assays showed that there was ~5- to 20-fold less kinase activity associated with immunoprecipitated Cbk1-Myc from either *mob2Δ*, *tao3Δ*, *hym1Δ*, or *kic1Δ* cells than from *ace2Δ* and wild-type cells (Figure 5). We obtained similar data from immunoprecipitants of asynchronous cells (our

unpublished data). Thus, Mob2p, Tao3p, Hym1p, and Kic1p are essential for maximal Cbk1p kinase activity, suggesting that they function in concert with Cbk1p or before Cbk1p in RAM network signaling. In contrast, Cbk1p kinase activation does not require Ace2p, which is consistent with Ace2p being a downstream target of RAM signaling.

Network of Hym1p, Cbk1p, Tao3p, Kic1p, and Mob2p Protein-Protein Interactions

To test for pairwise protein interactions between RAM network components, we performed two-hybrid assays on various fragments of these proteins (Figure 6A). We confirmed previously demonstrated Mob2p-Cbk1p and Tao3p-Cbk1p interactions (Racki *et al.*, 2000; Du and Novick, 2002; Weiss *et al.*, 2002) and observed Cbk1p-Cbk1p, Cbk1p-Kic1p, Tao3p-Kic1p, and Hym1p-Kic1p interactions (Figure 6A). We corroborated the Hym1p-Kic1p two-hybrid interactions by coimmunoprecipitating epitope-tagged proteins from asynchronous cells (Figure 6B).

Table 3. Mutations in RAM genes result in axial and bipolar budding defects

	Axial, %	Bipolar, %	Random, %
wt (vector)	3.0 ± 2.6	68.4 ± 1.4	28.6 ± 3.9
wt (<i>pBUD4</i>)	82.7 ± 2.0	4.5 ± 1.3	12.8 ± 3.0
<i>hym1</i>	59.2 ± 0.5	3.1 ± 1.6	38.1 ± 1.2
<i>cbk1</i>	54.6 ± 2.1	1.0 ± 0.1	44.4 ± 2.0
<i>tao3</i>	56.1 ± 2.9	3.1 ± 0.6	40.8 ± 2.3
<i>kic1</i>	40.1	2.3	57.7
<i>mob2</i>	43.6	3.9	52.5
<i>bni1</i>	85.9 ± 4.0	0.6 ± 0.5	13.6 ± 3.6
wt (vector)	0.0 ± 0.0	70.1 ± 2.6	29.9 ± 2.6
wt (<i>pBUD4</i>)	0.0 ± 0.0	75.8 ± 3.7	24.2 ± 3.7
<i>hym1/hym1</i>	1.0 ± 1.7	7.0 ± 2.6	92.0 ± 4.0
<i>cbk1/cbk1</i>	0.0 ± 0.0	8.6 ± 1.9	91.3 ± 2.0
<i>tao3/tao3</i>	0.3 ± 0.6	12.9 ± 3.0	86.8 ± 3.3
<i>bni1/bni1</i>	0.0 ± 0.0	9.6 ± 3.2	90.4 ± 3.2

Strains containing plasmid p2698 with *BUD4* (*pBUD4*) or pRS316 (vector) were grown to midlogarithmic phase, sonicated for cell separation and stained with Calcofluor to visualize bud scars. Strains contain *pBUD4* unless otherwise indicated. Upper rows show haploid strains, lower rows show diploid strains. For each sample, a minimum of 100 cells was counted from at least three independent fields. The strains used were wild-type (W303-1A and Y1028), *hym1*Δ (Y1614 and Y1622), *cbk1*Δ (Y1747 and Y2623), *tao3*Δ (Y3152 and Y3565), *kic1*Δ (Y3323 and Y3529), *mob2*Δ (Y3424 and Y3527), and *bni1*Δ (Y581 and Y2619).

Additional protein interactions were identified in a parallel study (Ho *et al.*, 2002). In these experiments, overproduced FLAG epitope-tagged Hym1p, Cbk1p, and Mob2p were immunoprecipitated from yeast extracts and the coprecipitated proteins were identified by mass spectroscopy. Tao3p, Mob2p, Ace2p, and Ssd1p, a protein implicated in Sit4p phosphatase function and polarized morphogenesis (Sutton *et al.*, 1991), copurified with Cbk1p, and Cbk1p copurified with Mob2p. The Cbk1p–Ssd1p interaction is likely to be functionally relevant, because deletion of the *SSD1* gene suppresses the lethality associated with disruption of RAM network signaling in certain strain backgrounds (Du and Novick, 2002; Jorgensen *et al.*, 2002). The various interaction data are summarized in Figure 6C. This complex network of interactions is reminiscent of other signal transduction pathways, such as the yeast pheromone response pathway (Schultz *et al.*, 1995; Elion, 2000; Dohlman and Thorner, 2001).

Sog2p Is a Novel RAM Component

To identify additional RAM-associated proteins, we conducted a two-hybrid screen by using Hym1p as bait and identified *YOR353c* as a gene encoding a Hym1p-interacting protein. *YOR353c* is registered as *SOG2* in the *Saccharomyces* Genome Database (<http://www.yeastgenome.org>) and is designated as such throughout this manuscript. *SOG2* encodes an 87-kDa protein that contains leucine-rich repeats and shares weak similarity with the NH₂-terminal region of *S. cerevisiae* adenylate cyclase. In parallel studies, *Sog2p* was found to coprecipitate with Cbk1p and Hym1p by large-

scale precipitation methods (Ho *et al.*, 2002) and to interact with Cbk1p in independent two-hybrid screens (Uetz *et al.*, 2000; Ito *et al.*, 2001).

To investigate whether *Sog2p* functions similarly to other RAM proteins, we analyzed the phenotypes of *sog2*Δ cells. *SOG2* and the RAM genes are essential for viability in the S288C-derived strains used for the *Saccharomyces* genome deletion project (Winzeler *et al.*, 1999). However, *SOG2* and the RAM genes were not essential for viability in our laboratory isolates of S288C and W303 strains, which carry the defective *ssd1-d* allele (Figure 7; our unpublished data). Using these strains, we found that cells lacking *SOG2* exhibited round morphologies and failed to separate upon completion of mitosis (Figure 7A). Moreover, *sog2*Δ cells were unable to restrict Ace2p to the daughter cell nucleus (Figure 7A). To determine whether *Sog2p* is important for Cbk1p kinase activity, as are Mob2p, Hym1p, Tao3p, and Kic1p (Figure 5), we conducted in vitro kinase assays of immunoprecipitated Cbk1p derived from *sog2*Δ cells. We found that Cbk1p kinase activity was greatly diminished in the *sog2*Δ cells, indicating that Mob2p–Cbk1p function was dependent on *Sog2p* (Figure 7B). These data indicate that *Sog2p* is an essential component of the RAM network.

Tao3p, *Hym1p*, *Sog2p*, and *Kic1p* Localize to Sites of Polarized Growth and Control Mob2p–Cbk1p Nuclear Localization

We examined the subcellular localizations of GFP-tagged RAM proteins to gain insight to their functional specificity. Indeed, consistent with roles in both polarized growth and Ace2p regulation, Cbk1p and Mob2p localize to the cortex during apical bud growth and to the bud neck and daughter cell nucleus during late mitosis (Colman-Lerner *et al.*, 2001; Weiss *et al.*, 2002). Tao3p was also shown to localize to sites of polarized growth but was not observed in the daughter nucleus (Du and Novick, 2002). We confirmed these observations by monitoring cells expressing Tao3-GFP (Figure 8A). Similarly, Kic1-GFP, Hym1-GFP, and *Sog2*-GFP localized prominently to incipient bud sites and small buds and weakly to the cortex and bud necks of large budded cells (Figure 8A). Tao3p, Hym1p, *Sog2p*, and Kic1p also localized to the growing tips of mating projections (Figure 8B), as shown for Mob2p and Cbk1p (Weiss *et al.*, 2002). We did not detect Tao3p, Hym1p, *Sog2p*, or Kic1p in the nucleus. Thus, because Mob2p and Cbk1p are the only proteins of the network that are detected in the daughter cell nucleus, it is likely that Mob2p and Cbk1p function downstream of the other RAM proteins with respect to Ace2p regulation.

Interdependency of RAM Protein Localization

To determine whether Cbk1p, Mob2p, Tao3p, Hym1p, *Sog2p*, and Kic1p are interdependent for localization, we systematically examined the localization of each protein in various RAM deletion strains. The results are summarized in Table 4.

We asked whether Mob2p and Cbk1p localization was dependent on other RAM proteins. As observed previously (Weiss *et al.*, 2002), Cbk1p and Mob2p localized interdependently at the cortex, bud neck, and daughter cell nucleus. In contrast, both Cbk1p and Mob2p were

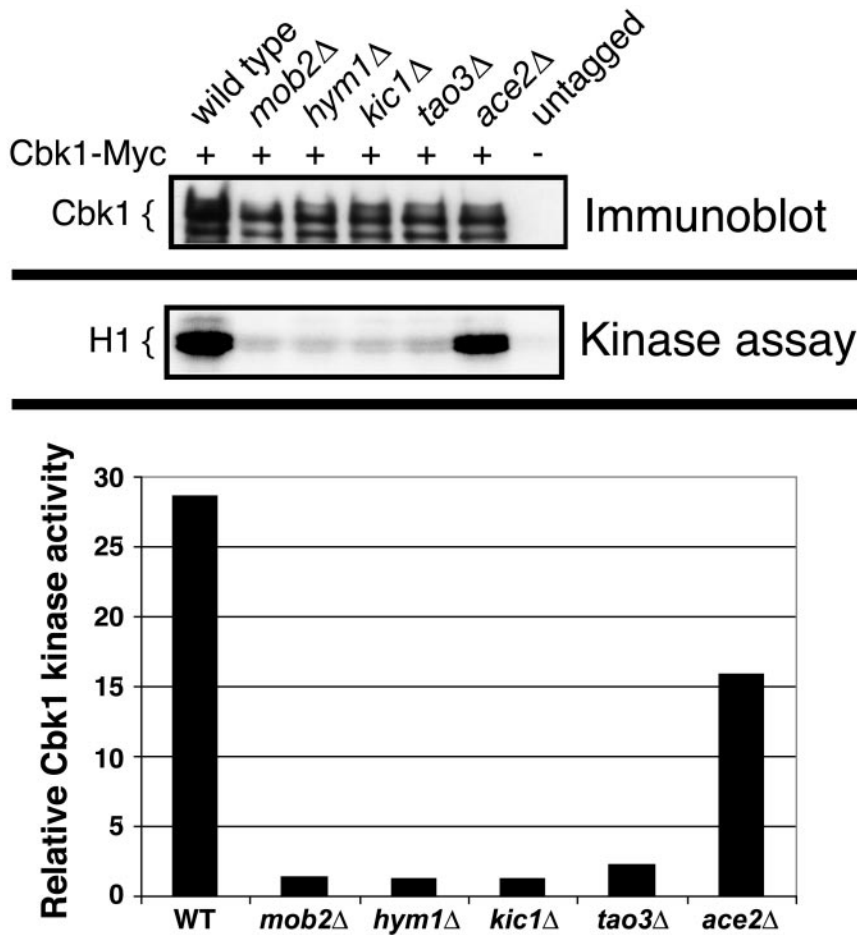


Figure 5. Cbk1p kinase activity is dependent on Mob2p, Hym1p, Kic1p, and Tao3p. Top, immunoblot of Cbk1-Myc immunoprecipitated from mating pheromone-treated wild-type (Y3280), *mob2Δ* (Y4035), *hym1Δ* (Y4032), *kic1Δ* (Y4034), *tao3Δ* (Y4033), *ace2Δ* (FLY1268), or untagged cells (W303-1A). The immunoblot was probed with anti-Myc antibody (9E10). Middle, an autoradiograph of the corresponding histone H1 kinase assays. The bottom panel shows graph of relative kinase activity. The Cbk1p-dependent histone H1 kinase activity from untagged cells was normalized to zero. The data from one of five experiments are presented; each experiment showed similar results. The maximal Cbk1p kinase activities in wild-type and *ace2Δ* cells are variable from experiment to experiment; thus, the apparent difference between kinase activities of wild-type and *ace2Δ* cells in the presented experiment is not significant.

able to localize to the bud cortex and bud neck in *tao3Δ*, *hym1Δ*, *sog2Δ*, and *kic1Δ* cells (Figure 9, A and B). Nevertheless, the nuclear localization of Mob2p and Cbk1p was distinctly aberrant in these cells. Mob2p was not detected in any *kic1Δ* or *hym1Δ* cell nucleus but was weakly detectable in (~9%) daughter nuclei or in (~9%) both mother and daughter nuclei of large budded *sog2Δ* cells (Figure 9B, arrows). Cbk1p was also undetectable in *kic1Δ* and *sog2Δ* cell nuclei but localized weakly to the daughter cell nucleus (~7%) or to both mother and daughter cell nuclei (~15%; see arrows Figure 9A) in some large budded *hym1Δ* cells. Cbk1p and Mob2p also localized to both mother and daughter cell nuclei in ~25–46% of the large budded *tao3Δ* cells (Figure 2A, inset) and to the daughter nucleus in only ~15% of the large budded *tao3Δ* cells. In particular, Mob2p was detectable in some late G1 *tao3Δ* cell nuclei (see arrowhead, Figure 9B, inset), which is in contrast to its localization in wild-type cells where Mob2p disappears from the daughter nucleus in early G1, well before bud emergence (Weiss *et al.*, 2002). Together, these findings support a model in which Kic1p, Sog2p, Hym1p, and Tao3p function upstream of Mob2p-Cbk1p to control the catalytic activity and proper nuclear localization of the Mob2p-Cbk1p complex.

There were subtle, but significant changes in RAM protein localization in *mob2Δ* and *cbk1Δ* cells. In these cells, Tao3-GFP, Hym1-GFP, Sog2-GFP, and Kic1-GFP seemed brighter at the cortices of small and large buds than in wild-type cells (Figure 9, C–F). Moreover, there were significantly fewer large budded *mob2Δ* and *cbk1Δ* cells with Kic1-GFP (0%), Hym1-GFP (11–14%), or Sog2-GFP (4–6%) localized to bud necks than in wild-type cells (49%, $n \geq 50$ large budded cells). Immunoblots of the RAM deletion strains reveal no significant difference in protein levels of the remaining RAM proteins (our unpublished data). Thus, these data suggest that Mob2p and Cbk1p influence the localized concentration or abundance of RAM proteins at the sites of polarized growth.

If Hym1p, Sog2p, and Kic1p are functionally linked as suggested by their binding interactions, then they may influence each other's subcellular distributions, as shown for Mob2p and Cbk1p (Weiss *et al.*, 2002). Indeed, Hym1-GFP and Sog2-GFP mislocalized from the cortex and bud neck in *kic1Δ* cells and instead localized diffusely to the cytoplasm (Figure 9, D and F). Hym1p similarly mislocalized to the cytoplasm in *sog2Δ* cells, but localized normally in *tao3Δ* cells. Strikingly, Kic1p localization was severely diminished at the cortex or bud neck in *sog2Δ*

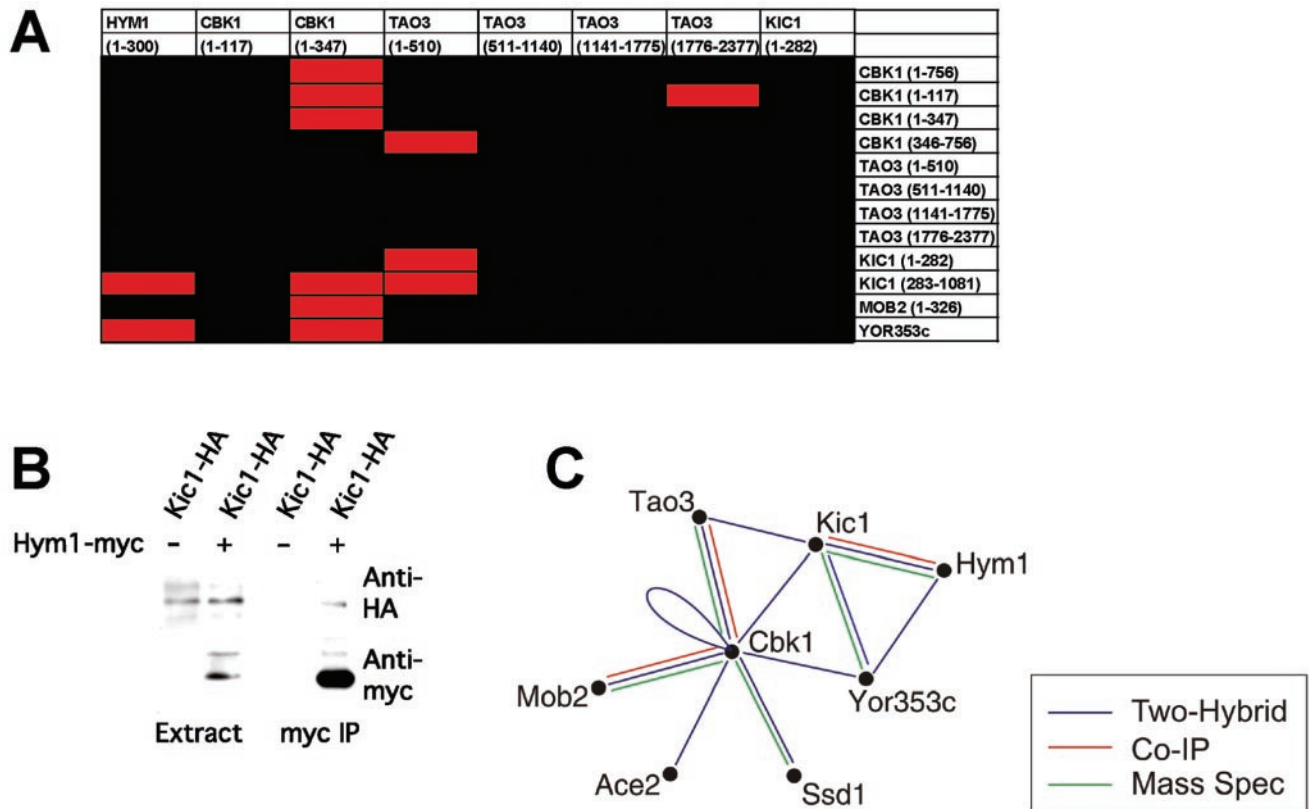
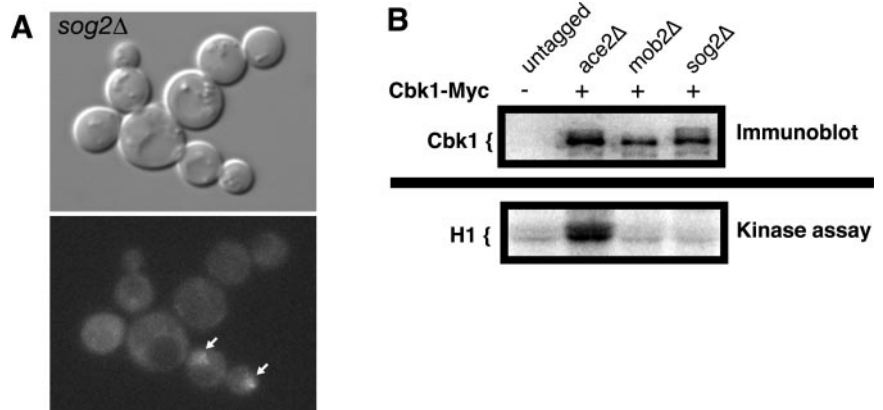


Figure 6. RAM protein interaction network. (A) Pairwise two-hybrid qualitative LacZ assays were performed among the various RAM proteins. The corresponding amino acid regions of each protein are noted in parentheses. Red boxes indicate a positive interaction; black boxes indicate no interaction. (B) Coimmunoprecipitation of Kic1-HA with Hym1-Myc. Extracts prepared from cells expressing Hym1-Myc or untagged Hym1p were immunoprecipitated with anti-Myc. Immunoprecipitated proteins were detected by immunoblot analysis with antibodies directed against HA (top) or Myc (bottom). Strains used were Kic1-HA Hym1-Myc (Y4089) and Kic1-HA (Y3615). (C) Summary of the RAM protein interaction network based on our data and that of others (Racki *et al.*, 2000; Ito *et al.*, 2001; Du and Novick, 2002; Ho *et al.*, 2002; Weiss *et al.*, 2002). YOR353c = SOG2.

cells, whereas Kic1p localization was normal in *hym1Δ* cells. In *tao3Δ* cells, the pattern of Kic1p localization was normal but seemed slightly diminished (Figure 9E). Sog2p

distribution was normal in *hym1Δ* and *tao3Δ* cells, as was Tao3p in *hym1Δ*, *sog2Δ*, and *kic1Δ* cells (Figure 9, C and F). These data indicate that Hym1p localization requires both

Figure 7. Sog2p is required for proper Ace2p localization, cell morphogenesis, and Cbk1p kinase activity. (A) Logarithmically growing *sog2Δ* (FLY1470) cells expressing Ace2-GFP were visualized by differential interference contrast microscopy (top) and fluorescence microscopy (bottom). Arrows point to Ace2-GFP in the nuclei of representative cells. (B) Top, immunoblot of Cbk1-Myc immunoprecipitated from mating pheromone-treated untagged cells (W303-1A), *ace2Δ* (FLY1268), *mob2Δ* (Y4035), and *sog2Δ* cells (FLY1492). The immunoblot was probed with anti-Myc antibody (9E10). Bottom, an autoradiograph of the corresponding histone H1 kinase assays. The relative kinase activity of immunoprecipitated Cbk1p from *sog2Δ* and *mob2Δ* cells was as low as immunoprecipitated kinase activity from untagged cells and was ~10-fold less than from *ace2Δ* cells. Similar data was obtained from asynchronous cells (our unpublished data).



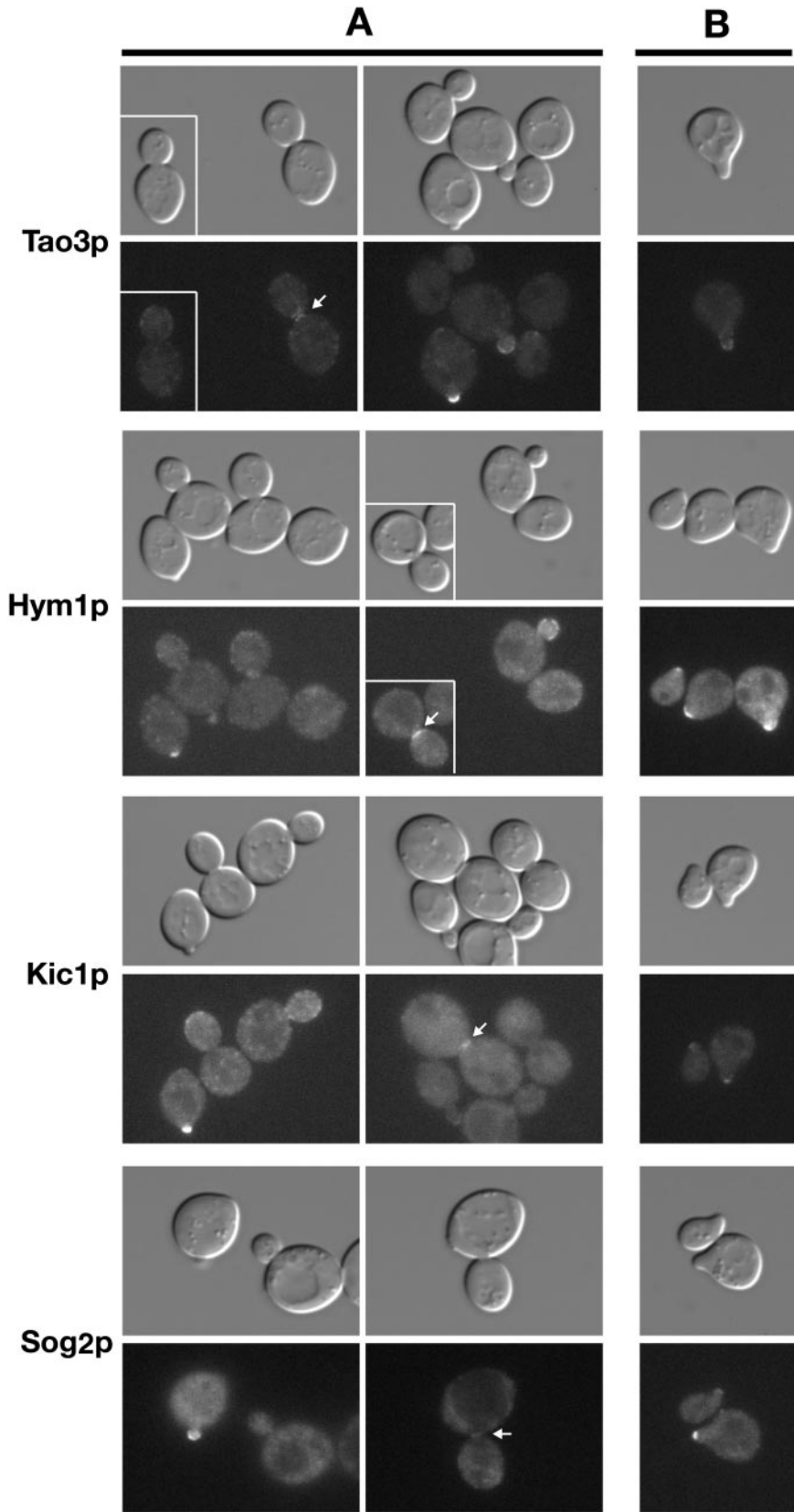


Figure 8. Tao3p, Hym1p, Kic1p, and Sog2p localize to sites of polarized growth. (A) Log-arithmetically growing homozygous diploid strains expressing Tao3-GFP (FLY1267), Hym1-GFP (FLY1244), Kic1-GFP (FLY1258), and Sog2-GFP (FLY1382) were visualized by differential interference contrast or fluorescence microscopy. Arrows point to bud neck localizations. (B) Tao3-GFP, Hym1-GFP, Kic1-GFP, and Sog2-GFP proteins localize to the tips of the mating projections upon pheromone treatment. *MATa* cells (FLY1263, FLY891, FLY947, and FLY1347) were treated with 5 μ M mating pheromone for 2 h before visualization. All images were captured and processed identically.

Table 4. Summary of RAM protein localization in wild type and mutant cells

	Cbk1p	Mob2p	Tao3p	Hym1p	Kic1p	Sog2p
WT	B N DN	B N DN	B N	B N	B N	B N
<i>cbk1Δ</i>		cytoplasm ^a	B ⁺ N	B ⁺ N	B ⁺	B ⁺ N
<i>mob2Δ</i>	M+DN ^a		B ⁺ N	B ⁺ N	B ⁺	B ⁺ N
<i>tao3Δ</i>	B N M+DN	B N M+DN		B N	B– N–	B N
<i>hym1Δ</i>	B N M+DN	B N	B N		B N	B ⁺ N
<i>kic1Δ</i>	B N	B N	B N	cytoplasm		cytoplasm
<i>sog2Δ</i>	B N	B N M+DN	B N	cytoplasm	cytoplasm ^b	

B, bud cortex; B⁺, B–, stronger or weaker cortical localization than in wild type cells; DN, daughter cell nucleus; M+DN, mother and daughter cell nuclei. N, bud neck during late mitosis; WT, wild type cells; See results for detailed description.

^a Weiss *et al.* 2002.

^b A greatly diminished amount of Kic1p can be detected on the cortex in some *sog2Δ* cells.

Sog2p and Kic1p and that Sog2p and Kic1p are interdependent for localization.

DISCUSSION

Cbk1p, Mob2p, Tao3p, Hym1p, Sog2p, and Kic1p Function in a Common Signaling Network

We present several lines of evidence that Cbk1p, Mob2p, Hym1p, Tao3p, Sog2p, and Kic1p function in a common signaling network, which we refer to as the RAM network. Cells deleted for each RAM gene exhibit dramatic cell separation defects, reduced mating efficiency and are rounder in morphology than wild-type cells. In addition *cbk1Δ*, *mob2Δ*, *tao3Δ*, *hym1Δ*, and *kic1Δ* mutants display indistinguishable defects in bud site selection and pheromone-induced polarized morphogenesis. There are no additive effects of RAM mutations, which further suggests the RAM proteins function in a common pathway (Figure 3; our unpublished data). Moreover, the RAM proteins form a complex network of protein–protein interactions and localize similarly to cortical sites of polarized growth during budding and cell separation, with some proteins dependent upon one another for localization. Although the combined results of previous studies regarding Mob2p, Cbk1p, Tao3p, and Hym1p anticipated the existence of a common signaling network that controls morphogenesis and cell separation (Dorland *et al.*, 2000; Racki *et al.*, 2000; Bidlingmaier *et al.*, 2001; Colman-Lerner *et al.*, 2001; Du and Novick, 2002; Weiss *et al.*, 2002), this study firmly establishes and defines the RAM network. Significantly, we have elucidated the *in vivo* relationships between the RAM proteins and have demonstrated that Kic1p kinase and the LRR-containing Sog2p are key components of the RAM network.

The Role of RAM Network in Regulating Ace2p Activity

It is apparent that the RAM network controls cell separation via regulation of the Ace2p transcription factor. Ace2p was previously shown to localize to the daughter nucleus at the end of mitosis and to activate daughter-specific transcription of a subset of genes important for septum degradation (Colman-Lerner *et al.*, 2001; Doolin *et al.*, 2001; Weiss *et al.*, 2002).

The RAM proteins Mob2p and Cbk1p also localize to the daughter cell nucleus at the end of mitosis and were shown to influence Ace2p function (Racki *et al.*, 2000; Bidlingmaier *et al.*, 2001; Colman-Lerner *et al.*, 2001; Weiss *et al.*, 2002). Herein, we demonstrate that deletion of the RAM genes *CBK1*, *MOB2*, *TAO3*, *HYM1*, *SOG2*, or *KIC1* cause indistinguishable defects in Ace2p localization and function. Specifically, in the deletion mutants, Ace2p is not restricted to the daughter cell nucleus at the end of mitosis, but instead enters both nuclei (Figures 1 and 7). Previous data suggest that Mob2p–Cbk1p kinase activity is necessary for inhibition of Ace2p nuclear export from the daughter cell nucleus (Weiss *et al.*, 2002). Our microarray analyses reveal that RAM deletion strains are markedly reduced for expression of Ace2-regulated genes (Figure 2). Thus, RAM signaling is required to regulate both Ace2p localization and activity.

Ace2p seems to be regulated at multiple levels. Previous studies have shown that Ace2p nuclear import is inhibited by CDK phosphorylation (O’Conallain *et al.*, 1999), but activated by MEN-dependent signaling (Weiss *et al.*, 2002). Nevertheless, Ace2p activation cannot be solely regulated by nuclear import, because Ace2p can enter nuclei in RAM deletion mutants and yet remains inactive as a transcription factor. It has been suggested that Mob2p–Cbk1p phosphorylates Ace2p, or an associated protein, to prevent its nuclear export (Weiss *et al.*, 2002). Our data are consistent with this possibility. Of the six RAM network proteins, Mob2p and Cbk1p are the only ones detected in the daughter nucleus. Thus, Mob2p–Cbk1p may function late in the network, with respect to Ace2p activation, and may phosphorylate Ace2p (or an associated protein), thereby inhibiting Ace2p nuclear export and, at the same time, activating Ace2p.

RAM Signaling and Cell Polarity

The role of the RAM network in Ace2p regulation is distinct from its role in polarized growth. Notably, *ace2Δ* cells are not defective in polarized growth (Racki *et al.*, 2000; Bidlingmaier *et al.*, 2001), and moderate overexpression of *ACE2* on high copy plasmids suppresses the cell separation but not the polarized growth defects of *cbk1Δ*, *mob2Δ*, *tao3Δ*, *hym1Δ*, and *kic1Δ* cells (Racki *et al.*, 2000; Colman-Lerner *et al.*, 2001; our unpublished data). The RAM network likely contributes to polarized growth by regulating actin-based secretion. Po-

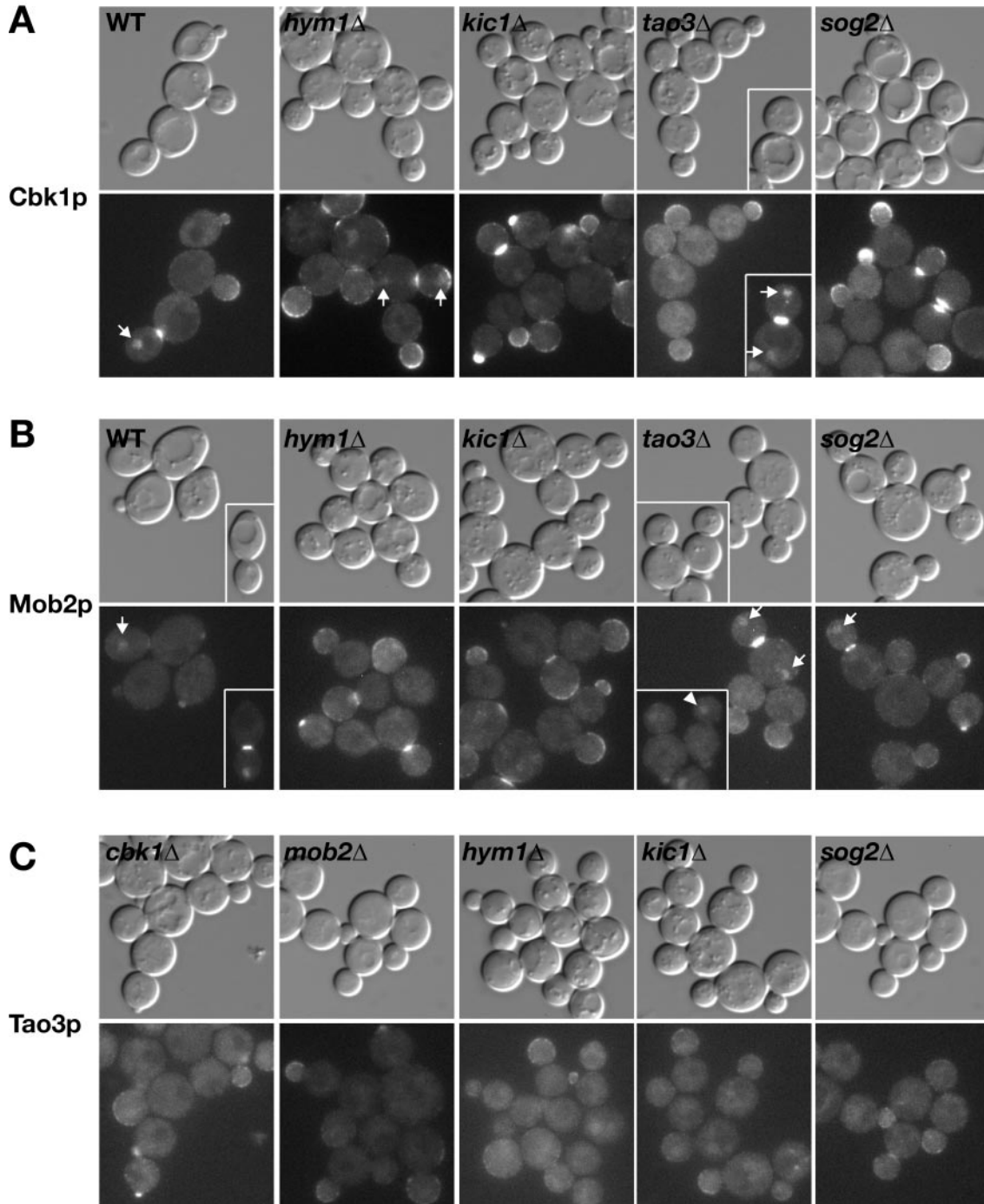


Figure 9. Relationship between Cbk1p, Mob2p, Tao3p, Hym1p, Kic1p, and Sog2p for protein localization. Logarithmically growing cells expressing GFP-tagged proteins were visualized by differential interference contrast and fluorescence microscopy. (A) Localization of Cbk1-GFP in wild-type (FLY895), *hym1* Δ (FLY1383), *kic1* Δ (FLY1344), *tao3* Δ (FLY1259), and *sog2* Δ cells (FLY1515). Arrows point to nuclear localization of Cbk1-GFP in late mitotic cells. (B) Localization of Mob2-GFP in wild-type (FLY893), *hym1* Δ (FLY1342), *kic1* Δ (FLY1343), *tao3* Δ (FLY1260) and *sog2* Δ (FLY1499) cells. Arrows point to nuclear localization of Mob2-GFP. The arrowhead points to a G1 *tao3* Δ cell (inset) with Mob2-GFP in the nucleus. (C) Localization of Tao3-GFP in *cbk1* Δ (FLY1324), *mob2* Δ (FLY1386), *hym1* Δ (FLY1326), *kic1* Δ (FLY1325), and *sog2* Δ (FLY1500) cells. (D) Localization of Hym1-GFP in *cbk1* Δ (FLY1246), *mob2* Δ (FLY1245), *kic1* Δ (FLY1261), *tao3* Δ (FLY1262), and *sog2* Δ (FLY1514) cells. (E) Localization of Kic1-GFP in *cbk1* Δ (FLY1248), *mob2* Δ (FLY1247), *hym1* Δ (FLY1278), *tao3* Δ (FLY1249), and *sog2* Δ (FLY1465) cells. (F) Localization of Sog2-GFP in *cbk1* Δ (FLY1475), *mob2* Δ (FLY1474), *hym1* Δ (FLY1472), *kic1* Δ (FLY1471), and *tao3* Δ (FLY1473) cells. Immunoblots of the deletion strains reveal no significant differences in RAM protein levels (our unpublished data). Each image was captured and processed identically.

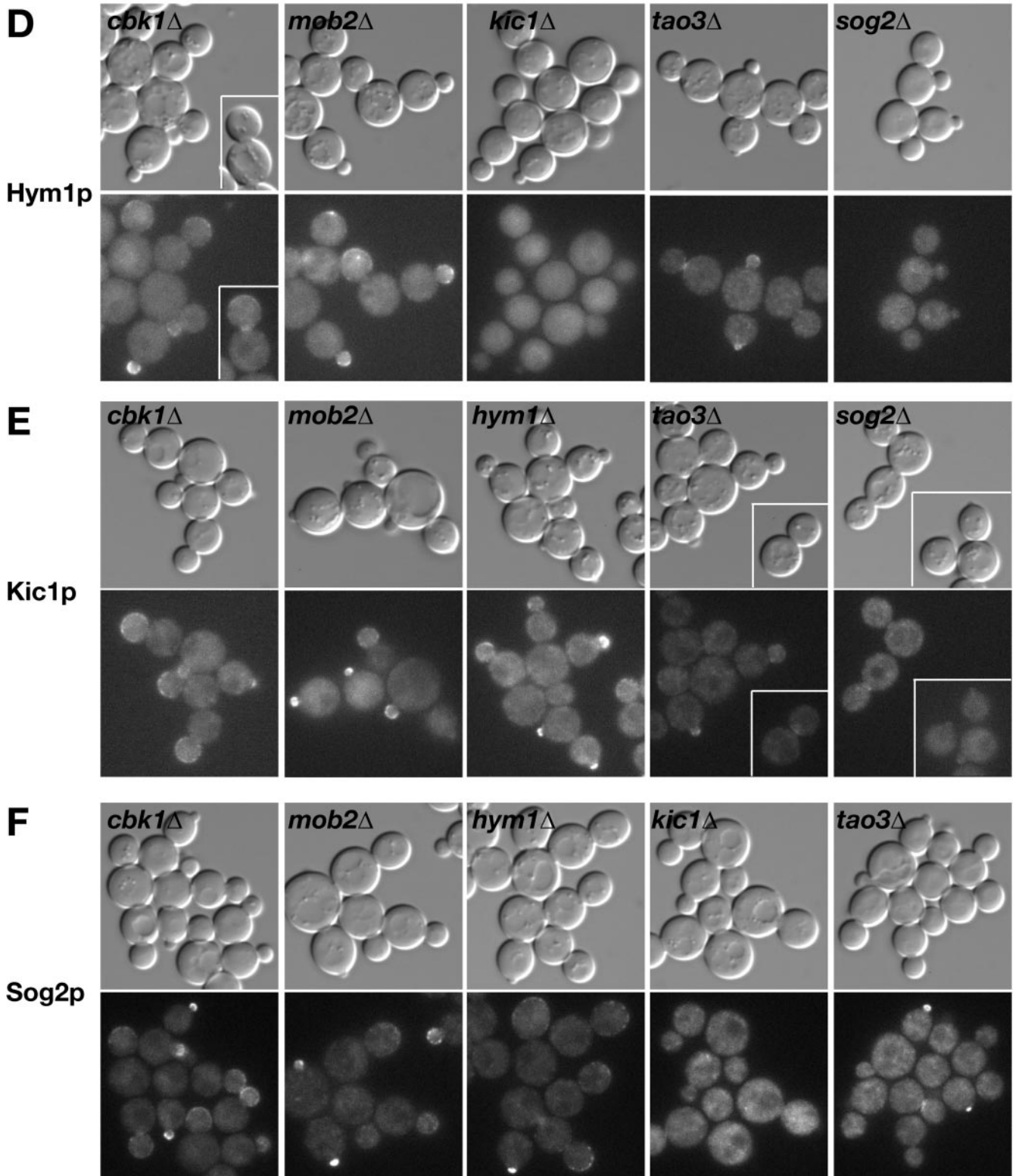


Figure 9 (cont).

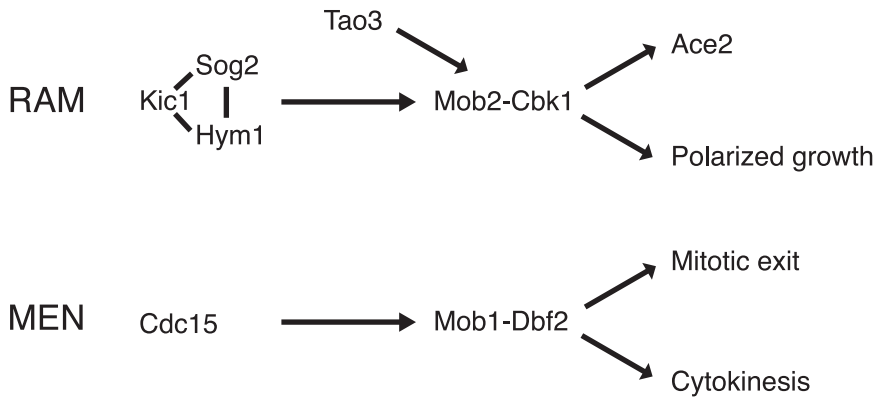


Figure 10. Models of conserved regulatory MEN and RAM networks in yeast. The Mob2p–Cbk1p kinase complex likely functions late in the RAM network because 1) Cbk1p kinase activity is dependent on all known RAM proteins, and 2) Mob2p and Cbk1p are the only RAM proteins detectable in the daughter cell nucleus at the end of mitosis. Kic1p, Sog2p, and Hym1p may function together as a complex because Hym1p binds Sog2p and Kic1p and is Sog2p- and Kic1p-dependent for localization. By analogy to the MEN protein Cdc15p, which activates the Mob1p–Dbf2p kinase complex *in vitro*, Kic1p may phosphorylate and activate the Mob2p–Cbk1p complex. Tao3p is a 270-kDa protein of unknown function that interacts with Cbk1p and Kic1p. Thus, Tao3p may serve as a scaffold that facilitates activation of Mob2p–Cbk1p kinase by Kic1p.

larized actin cables seem to act as tracks that guide myosin motors carrying cargo of secretory vesicles containing materials necessary for cell surface expansion. The yeast formin, Bni1p controls the assembly and polarization of actin cables (Burns *et al.*, 1994; Evangelista *et al.*, 2002), and a *bni1Δ* deletion mutation results in defects in cable assembly and polarization, leading to general defects in cell polarization (Evangelista *et al.*, 2002). In contrast to *bni1Δ* cells, the actin cables seem relatively normal in *cbk1Δ*, *mob2Δ*, *tao3Δ*, *hym1Δ*, and *kic1Δ* cells (Bidingmaier *et al.*, 2001; Du and Novick, 2002; Weiss *et al.*, 2002; our unpublished data). Furthermore, the role of RAM signaling in maintenance of cell polarity seems distinct from that of Bni1p, because deletion of RAM genes in combination with *bni1Δ* results in a synergistic defect in mating projection formation. Perhaps the RAM network operates at the level of vesicle transport or exocyst function (TerBush *et al.*, 1996; Lipschutz and Mostov, 2002). Consistent with this idea, Cbk1p was shown to bind Sec2p, a guanine nucleotide exchange factor required for vesicle transport and exocytosis, in a two-hybrid assay (Racki *et al.*, 2000).

Order of RAM Protein Function

By analogy to the *S. cerevisiae* MEN (Bardin and Amon, 2001), it seems plausible that Kic1p kinase activates the Mob2p–Cbk1p complex directly (Figure 10). Recombinant Kic1p-related Cdc15p kinase was shown to phosphorylate and activate the Mob2p–Cbk1p-related Mob1p–Dbf2p kinase complex (Mah *et al.*, 2001). The presence of Kic1p in the RAM network suggests a similar mechanism for the Mob2p–Cbk1p kinase activation. Consistent with this hypothesis, we have shown that Mob2p–Cbk1p kinase activity is dependent on Kic1p.

Hym1p, Sog2p, and Tao3p are not related to known MEN components, yet are also required for Mob2–Cbk1p kinase activation. What might be their molecular functions? Our data indicate that Hym1p, Sog2p and Kic1p are functionally linked. Hym1p coimmunoprecipitates with Kic1p and mislocalizes in the absence of Kic1p or Sog2p. Moreover, Sog2p, which associates with Hym1p, Cbk1p, and Kic1p (Figure 6) (Ho *et al.*, 2002), is interdependent with Kic1p for localization. Curiously, Kic1p and Sog2p localize to the bud cortex independently of Hym1p, suggesting that Kic1p and Sog2p

function upstream of Hym1p or that Sog2p mediates the association of Hym1p with Kic1p. Hym1p and Sog2p may regulate Kic1p kinase activity or mediate interactions between Kic1p kinase and its substrates. Along these lines, Hym1p and Sog2p might stabilize Kic1p and Mob2p–Cbk1p interactions for Cbk1p kinase activation.

Tao3p is a large 270-kDa protein that interacts with Cbk1p and Kic1p (Figure 6; Du and Novick, 2002) that may also facilitate Mob2p–Cbk1p kinase activation by Kic1p. Moreover, Tao3p may be important for regulating the timing or duration of Mob2p–Cbk1p nuclear localization, because Mob2p and Cbk1p seem to remain localized to the nuclei for a longer duration in some *tao3Δ* cells than in wild-type cells (arrows Figure 9, A and B).

Although Tao3p, Hym1p, Sog2p, and Kic1p all seem to act upstream of Mob2p–Cbk1p with respect to Cbk1p kinase activation, it is not yet possible to definitively order their functions with respect to each other. Indeed, it is probable that the RAM network is not linear. In support, we have found that Hym1p, Sog2p, Kic1p, and Tao3p are more prominent at the bud cortex in the absence of Mob2p or Cbk1p. Thus, in addition to acting late in the RAM network, Mob2–Cbk1p may regulate Hym1p, Sog2p, Kic1p, and Tao3p localization or stability, perhaps as part of a feedback mechanism.

Other RAM Proteins and Associated Proteins

It is likely that other RAM network components or associated proteins will be identified. True RAM components will be required for cell morphogenesis and Ace2p regulation, although some effectors or targets of RAM signaling may have additional or separable functions. Indeed, the nonessential protein Ssd1p was also shown to bind Cbk1p, suggesting that it may have a role in RAM regulation or may function as an effector of the RAM pathway (Racki *et al.*, 2000). Ssd1p was originally identified as a suppressor of mutation in Sit4p phosphatase (Sutton *et al.*, 1991). Recently, *ssd1Δ* mutations were shown to suppress the lethality associated with deletion of RAM genes (Du and Novick, 2002; Jorgensen *et al.*, 2002). These data suggest that Ssd1p negatively regulates a function that is essential in the absence of RAM signaling, and thus Ssd1p activity may be coordinated with RAM signaling.

RAM-like Signaling Networks Are Conserved

All of the components of the RAM network are conserved. In *Drosophila*, Cbk1p-related and Tao3p-like proteins were shown to be required to maintain the integrity of cellular extensions during morphogenesis (Geng *et al.*, 2000; Cong *et al.*, 2001). Similarly, *S. pombe* orthologs to Cbk1p, Mob2p, and Tao3p (designated Orb6p, Mob2p, and Mor2p) were shown to be essential for cell polarity and morphogenesis (Verde *et al.*, 1998; Hirata *et al.*, 2002; Hou *et al.*, 2003). Deletion of *S. pombe orb6*, *mob2*, or *mor2* genes cause a depolarization of the actin cytoskeleton resulting in striking spherical cell morphologies. Like their *S. cerevisiae* counterparts, the proteins encoded by *S. pombe orb6*, *mob2*, or *mor2* genes localize to the sites of polarized growth. However, unlike *S. cerevisiae* Mob2p and Cbk1p, *S. pombe* Orb6p and Mob2p were not observed to localize to the nucleus or to regulate a transcription factor.

We suspect that future work will demonstrate that the overall organization of the RAM-related signaling networks is conserved in all eukaryotes. Thus, in an effort to map a mammalian RAM-like signaling network, we identified several proteins associated with the human Kic1p-like kinase *Mst3* (Schinkmann and Blenis, 1997) (see Supplement). We found that *Mst3* coimmunoprecipitates with phocein (Luca and Winey, 1998; Baillat *et al.*, 2001; Moreno *et al.*, 2001), a distantly related Mob1p/Mob2p-related protein that is highly conserved in animal cells (see Supplement Figure S1). This work supports the idea that RAM-like signaling modules are conserved in mammalian cells; however, more work is necessary to elucidate the function of *Mst3* kinase complex and to identify other components of its signaling network.

Current evidence suggest that eukaryotic RAM and MEN signaling modules are important for regulating and coordinating a variety of important cellular processes, including mitotic exit, cytokinesis, cell polarity, gene transcription, and vesicle transport. In this sense, different RAM and MEN signaling networks can be likened to the different MAP kinase-signaling networks, which are compromised of conserved protein modules that affect different downstream processes (Posas *et al.*, 1998; Wilkinson and Millar, 2000). Further work is necessary regarding the identity, function, and targets of these novel classes of regulatory networks.

ACKNOWLEDGMENTS

We thank Christopher Roberts and Matthew Marton for help with the microarray analysis, and S. Kang for help with characterization of RAM pathway mutants. We also thank Eric Weiss, Chris Herbert, David Stillman, and members of the Luca and Boone laboratories for insightful discussions. This work was funded by grants from the National Institutes of Health (R01 GM-60575) to F.C.L.; Natural Sciences and Engineering Research Council, the National Cancer Institute of Canada to C.B.; and an Natural Sciences and Engineering Research Council graduate student fellowship to B.N.

REFERENCES

Amberg, D.C., Zahner, J.E., Mulholland, J.W., Pringle, J.R., and Botstein, D. (1997). Aip3p/Bud6p, a yeast actin-interacting protein that is involved in morphogenesis and the selection of bipolar budding sites. *Mol. Biol. Cell* 8, 729–753.

Andersen, S.S., and Bi, G.Q. (2000). Axon formation: a molecular model for the generation of neuronal polarity. *Bioessays* 22, 172–179.

Baillat, G., Moqrich, A., Castets, F., Baude, A., Bailly, Y., Benmerah, A., and Monneron, A. (2001). Molecular cloning and characterization of phocein, a protein found from the Golgi complex to dendritic spines. *Mol. Biol. Cell* 12, 663–673.

Bardin, A.J., and Amon, A. (2001). Men and sin: what's the difference? *Nat. Rev. Mol. Cell. Biol.* 2, 815–826.

Bidlingmaier, S., Weiss, E.L., Seidel, C., Drubin, D.G., and Snyder, M. (2001). The Cbk1p pathway is important for polarized cell growth and cell separation in *Saccharomyces cerevisiae*. *Mol. Cell. Biol.* 21, 2449–2462.

Boone, C., Davis, N.G., and Sprague, G.F., Jr. (1993). Mutations that alter the third cytoplasmic loop of the a-factor receptor lead to a constitutive and hypersensitive phenotype. *Proc. Natl. Acad. Sci. USA* 90, 9921–9925.

Burns, N., Grimwade, B., Ross-Macdonald, P.B., Choi, E.Y., Finberg, K., Roeder, G.S., and Snyder, M. (1994). Large-scale analysis of gene expression, protein localization, and gene disruption in *Saccharomyces cerevisiae*. *Genes Dev.* 8, 1087–1105.

Casamayor, A., and Snyder, M. (2002). Bud-site selection and cell polarity in budding yeast. *Curr. Opin. Microbiol.* 5, 179–186.

Chant, J., and Pringle, J.R. (1995). Patterns of bud-site selection in the yeast *Saccharomyces cerevisiae*. *J. Cell Biol.* 129, 751–765.

Chenevert, J., Valtz, N., and Herskowitz, I. (1994). Identification of genes required for normal pheromone-induced cell polarization in *Saccharomyces cerevisiae*. *Genetics* 136, 1287–1296.

Colman-Lerner, A., Chin, T.E., and Brent, R. (2001). Yeast Cbk1 and Mob2 activate daughter-specific genetic programs to induce asymmetric cell fates. *Cell* 107, 739–750.

Cong, J., Geng, W., He, B., Liu, J., Charlton, J., and Adler, P.N. (2001). The furry gene of *Drosophila* is important for maintaining the integrity of cellular extensions during morphogenesis. *Development* 128, 2793–2802.

DeRisi, J.L., Iyer, V.R., and Brown, P.O. (1997). Exploring the metabolic and genetic control of gene expression on a genomic scale. *Science* 278, 680–686.

Dohlman, H.G., and Thorner, J.W. (2001). Regulation of G protein-initiated signal transduction in yeast: paradigms and principles. *Annu. Rev. Biochem.* 70, 703–754.

Dohrmann, P.R., Butler, G., Tamai, K., Dorland, S., Greene, J.R., Thiele, D.J., and Stillman, D.J. (1992). Parallel pathways of gene regulation: homologous regulators SWI5 and ACE2 differentially control transcription of HO and chitinase. *Genes Dev.* 6, 93–104.

Doolin, M.T., Johnson, A.L., Johnston, L.H., and Butler, G. (2001). Overlapping and distinct roles of the duplicated yeast transcription factors Ace2p and Swi5p. *Mol. Microbiol.* 40, 422–432.

Dorland, S., Deegenars, M.L., and Stillman, D.J. (2000). Roles for the *Saccharomyces cerevisiae* SDS3, CBK1 and HYM1 genes in transcriptional repression by SIN3. *Genetics* 154, 573–586.

Du, L.L., and Novick, P. (2002). Pag1p, a novel protein associated with protein kinase Cbk1p, is required for cell morphogenesis and proliferation in *Saccharomyces cerevisiae*. *Mol. Biol. Cell* 13, 503–514.

Durfee, T., Becherer, K., Chen, P.L., Yeh, S.H., Yang, Y., Kilburn, A.E., Lee, W.H., and Elledge, S.J. (1993). The retinoblastoma protein associates with the protein phosphatase type 1 catalytic subunit. *Genes Dev.* 7, 555–569.

Elion, E.A. (2000). Pheromone response, mating and cell biology. *Curr. Opin. Microbiol.* 3, 573–581.

Evangelista, M., Blundell, K., Longtine, M.S., Chow, C.J., Adames, N., Pringle, J.R., Peter, M., and Boone, C. (1997). Bni1p, a yeast

- formin linking cdc42p and the actin cytoskeleton during polarized morphogenesis. *Science* 276, 118–122.
- Evangelista, M., Klebl, B.M., Tong, A.H., Webb, B.A., Leeuw, T., Leberer, E., Whiteway, M., Thomas, D.Y., and Boone, C. (2000). A role for myosin-I in actin assembly through interactions with Vrp1p, Bee1p, and the Arp2/3 complex. *J. Cell Biol.* 148, 353–362.
- Evangelista, M., Pruyne, D., Amberg, D.C., Boone, C., and Bretscher, A. (2002). Formins direct Arp2/3-independent actin filament assembly to polarize cell growth in yeast. *Nat. Cell Biol.* 4, 260–269.
- Fink, G.R., and Styles, C.A. (1972). Curing of a killer factor in *Saccharomyces cerevisiae*. *Proc. Natl. Acad. Sci. USA* 69, 2846–2849.
- Geng, W., He, B., Wang, M., and Adler, P.N. (2000). The tricorned gene, which is required for the integrity of epidermal cell extensions, encodes the *Drosophila* nuclear DBF2-related kinase. *Genetics* 156, 1817–1828.
- Gietz, R.D., and Sugino, A. (1988). New yeast-*Escherichia coli* shuttle vectors constructed with in vitro mutagenized yeast genes lacking six-base pair restriction sites. *Gene* 74, 527–534.
- Gulli, M.P., Jaquenoud, M., Shimada, Y., Niederhauser, G., Wiget, P., and Peter, M. (2000). Phosphorylation of the Cdc42 exchange factor Cdc24 by the PAK-like kinase Cla4 may regulate polarized growth in yeast. *Mol. Cell* 6, 1155–1167.
- Gyuris, J., Golemis, E., Chertkov, H., and Brent, R. (1993). Cdi1, a human G1 and S phase protein phosphatase that associates with Cdk2. *Cell* 75, 791–803.
- Hirata, D., *et al.* (2002). Fission yeast Mor2/Cps12, a protein similar to *Drosophila* Furry, is essential for cell morphogenesis and its mutation induces Wee1-dependent G(2) delay. *EMBO J.* 21, 4863–4874.
- Ho, Y., *et al.* (2002). Systematic identification of protein complexes in *Saccharomyces cerevisiae* by mass spectrometry. *Nature* 415, 180–183.
- Horecka, J., and Jigami, Y. (2000). Identifying tagged transposon insertion sites in yeast by direct genomic sequencing. *Yeast* 16, 967–970.
- Hou, M.C., Wiley, D.J., Verde, F., and McCollum, D. (2003). Mob2p interacts with the protein kinase Orb6p to promote coordination of cell polarity with cell cycle progression. *J. Cell Sci.* 116, 125–135.
- Hughes, T.R., *et al.* (2000). Functional discovery via a compendium of expression profiles. *Cell* 102, 109–126.
- Ito, T., Chiba, T., Ozawa, R., Yoshida, M., Hattori, M., and Sakaki, Y. (2001). A comprehensive two-hybrid analysis to explore the yeast protein interactome. *Proc. Natl. Acad. Sci. USA* 98, 4569–4574.
- Jorgensen, P., Nelson, B., Robinson, M.D., Chen, Y., Andrews, B., Tyers, M., and Boone, C. (2002). High-resolution genetic mapping with ordered arrays of *Saccharomyces cerevisiae* deletion mutants. *Genetics* 162, 1091–1099.
- Karos, M., and Fischer, R. (1999). Molecular characterization of HymA, an evolutionarily highly conserved and highly expressed protein of *Aspergillus nidulans*. *Mol. Gen. Genet.* 260, 510–521.
- Kilmartin, J.V., and Adams, A.E. (1984). Structural rearrangements of tubulin and actin during the cell cycle of the yeast *Saccharomyces*. *J. Cell Biol.* 98, 922–933.
- Knust, E. (2000). Control of epithelial cell shape and polarity. *Curr. Opin. Genet. Dev.* 10, 471–475.
- Leberer, E., Thomas, D.Y., and Whiteway, M. (1997). Pheromone signalling and polarized morphogenesis in yeast. *Curr. Opin. Genet. Dev.* 7, 59–66.
- Lew, D.J., and Reed, S.I. (1995). Cell cycle control of morphogenesis in budding yeast. *Curr. Opin. Genet. Dev.* 5, 17–23.
- Lipschutz, J.H., and Mostov, K.E. (2002). Exocytosis: the many masters of the exocyst. *Curr. Biol.* 12, R212–R214.
- Longtine, M.S., McKenzie, A., 3rd, Demarini, D.J., Shah, N.G., Wach, A., Brachat, A., Philippsen, P., and Pringle, J.R. (1998). Additional modules for versatile and economical PCR-based gene deletion and modification in *Saccharomyces cerevisiae*. *Yeast* 14, 953–961.
- Luca, F.C., Mody, M., Kurischko, C., Roof, D.M., Giddings, T.H., and Winey, M. (2001). *Saccharomyces cerevisiae* Mob1p is required for cytokinesis and mitotic exit. *Mol. Cell. Biol.* 21, 6972–6983.
- Luca, F.C., and Winey, M. (1998). MOB1, an essential yeast gene required for completion of mitosis and maintenance of ploidy. *Mol. Biol. Cell* 9, 29–46.
- Mah, A.S., Jang, J., and Deshaies, R.J. (2001). Protein kinase Cdc15 activates the Dbf2-Mob1 kinase complex. *Proc. Natl. Acad. Sci. USA* 98, 7325–7330.
- Miyamoto, H., Matsushiro, A., and Nozaki, M. (1993). Molecular cloning of a novel mRNA sequence expressed in cleavage stage mouse embryos. *Reprod. Dev.* 34, 1–7.
- Moreno, C.S., Lane, W.S., and Pallas, D.C. (2001). A mammalian homolog of yeast MOB1 is both a member and a putative substrate of striatin-family/protein phosphatase 2A complexes. *J. Biol. Chem.* 276, 23.
- O’Connell, C., Doolin, M.T., Taggart, C., Thornton, F., and Butler, G. (1999). Regulated nuclear localisation of the yeast transcription factor Ace2p controls expression of chitinase (CTS1) in *Saccharomyces cerevisiae*. *Mol. Gen. Genet.* 262, 275–282.
- Peter, M., Gartner, A., Horecka, J., Ammerer, G., and Herskowitz, I. (1993). FAR1 links the signal transduction pathway to the cell cycle machinery in yeast. *Cell* 73, 747–760.
- Phizicky, E.M., and Fields, S. (1995). Protein-protein interactions: methods for detection and analysis. *Microbiol. Rev.* 59, 94–123.
- Posas, F., Takekawa, M., and Saito, H. (1998). Signal transduction by MAP kinase cascades in budding yeast. *Curr. Opin. Microbiol.* 1, 175–182.
- Pruyne, D., and Bretscher, A. (2000a). Polarization of cell growth in yeast. *J. Cell Sci.* 113, 571–585.
- Pruyne, D., and Bretscher, A. (2000b). Polarization of cell growth in yeast. I. Establishment and maintenance of polarity states. *J. Cell Sci.* 113, 365–375.
- Pruyne, D., Evangelista, M., Yang, C., Bi, E., Zigmund, S., Bretscher, A., and Boone, C. (2002). Role of formins in actin assembly: nucleation and barbed-end association. *Science* 297, 612–615.
- Racki, W.J., Becam, A.M., Nasr, F., and Herbert, C.J. (2000). Cbk1p, a protein similar to the human myotonic dystrophy kinase, is essential for normal morphogenesis in *Saccharomyces cerevisiae*. *EMBO J.* 19, 4524–4532.
- Roberts, C.J., *et al.* (2000). Signaling and circuitry of multiple MAPK pathways revealed by a matrix of global gene expression profiles. *Science* 287, 873–880.
- Rupes, I. (2002). Checking cell size in yeast. *Trends Genet.* 18, 479–485.
- Sagot, I., Klee, S.K., and Pellman, D. (2002). Yeast formins regulate cell polarity by controlling the assembly of actin cables. *Nat. Cell Biol.* 4, 42–50.
- Schinkmann, K., and Blenis, J. (1997). Cloning and characterization of a human STE20-like protein kinase with unusual cofactor requirements. *J. Biol. Chem.* 272, 28695–28703.
- Schultz, J., Ferguson, B., and Sprague, G.F., Jr. (1995). Signal transduction and growth control in yeast. *Curr. Opin. Genet. Dev.* 5, 31–37.

- Sheu, Y.J., Barral, Y., and Snyder, M. (2000). Polarized growth controls cell shape and bipolar bud site selection in *Saccharomyces cerevisiae*. *Mol. Cell. Biol.* *20*, 5235–5247.
- Sheu, Y.J., Santos, B., Fortin, N., Costigan, C., and Snyder, M. (1998). Spa2p interacts with cell polarity proteins and signaling components involved in yeast cell morphogenesis. *Mol. Cell. Biol.* *18*, 4053–4069.
- Sullivan, D.S., Biggins, S., and Rose, M.D. (1998). The yeast centrin, cdc31p, and the interacting protein kinase, Kic1p, are required for cell integrity. *J. Cell Biol.* *143*, 751–765.
- Sutton, A., Immanuel, D., and Arndt, K.T. (1991). The SIT4 protein phosphatase functions in late G1 for progression into S phase. *Mol. Cell. Biol.* *11*, 2133–2148.
- TerBush, D.R., Maurice, T., Roth, D., and Novick, P. (1996). The Exocyst is a multiprotein complex required for exocytosis in *Saccharomyces cerevisiae*. *EMBO J.* *15*, 6483–6494.
- Uetz, P., *et al.* (2000). A comprehensive analysis of protein-protein interactions in *Saccharomyces cerevisiae*. *Nature* *403*, 623–627.
- Ugolini, S., and Bruschi, C.V. (1996). The red/white colony color assay in the yeast *Saccharomyces cerevisiae*: epistatic growth advantage of white *ade8–18, ade2* cells over red *ade2* cells. *Curr. Genet.* *30*, 485–492.
- Verde, F., Wiley, D.J., and Nurse, P. (1998). Fission yeast orb6, a ser/thr protein kinase related to mammalian rho kinase and myotonic dystrophy kinase, is required for maintenance of cell polarity and coordinates cell morphogenesis with the cell cycle. *Proc. Natl. Acad. Sci. USA* *95*, 7526–7531.
- Vink, E., Vossen, J.H., Ram, A.F., Van Den Ende, H., Brekelmans, S., De Nobel, H., and Klis, F.M. (2002). The protein kinase Kic1 affects 1,6-beta-glucan levels in the cell wall of *Saccharomyces cerevisiae*. *Microbiology* *148*, 4035–4048.
- Weiss, E.L., Kurischko, C., Zhang, C., Shokat, K., Drubin, D.G., and Luca, F.C. (2002). The *Saccharomyces cerevisiae* Mob2p-Cbk1p kinase complex promotes polarized growth and acts with the mitotic exit network to facilitate daughter cell-specific localization of Ace2p transcription factor. *J. Cell Biol.* *158*, 885–900.
- Wilkinson, M.G., and Millar, J.B. (2000). Control of the eukaryotic cell cycle by MAP kinase signaling pathways. *FASEB J.* *14*, 2147–2157.
- Winzeler, *et al.* (1999). Functional characterization of the *S. cerevisiae* genome by gene deletion and parallel analysis. *Science* *285*, 901–906.